# Synthesis and Electrochemistry of Biodegradable Ligands-Iminodiglutaric acid and Iminoglutaricsuccinic acid-and their Complexes with Selected Metal Ions ($Zn^{2+}$, $Cd^{2+}$, $Cu^{2+}$)

By

**Yonas Yohannes Desta**

Thesis presented in partial fulfillment for the degree of

**Magister Scientiae**
(Chemistry/Chemie)

at the Faculty of Science at the University of Stellenbosch,
Republic of South Africa

Supervisor: Prof. Andrew M. Crouch
Co-Supervisor Dr. M. W. Bredenkamp

December 2004

# Declaration

I, the undersigned, hereby declare that the work contained in this thesis is my own original work and that I have not previously in its entirety or in part submitted it at any university for a degree.

# Abstract

Two new potentially biodegradable aminopolycarboxylic acid ligands, iminodiglutaric acid tetra sodium salt (IDG-4Na) and iminoglutaricsuccinic acid tetra sodium salt (IGS-4Na), were synthesized in reasonably good yield and purity. The commercially unavailable precursor for the two ligands, ethyl β-aminoglutarate, was synthesised in high yield and purity, and together with the two ligands were fully characterized by means of melting point measurements and various spectrometric techniques ($^{1}$H-NMR, $^{13}$C-NMR, MS and IR).

For the first time, an electrochemical study has been conducted on the complexes of these ligands with selected transition metal ions ($Zn^{2+}$, $Cu^{2+}$ and $Cd^{2+}$). An electrochemical technique, cyclic voltammetry (CV), was utilized on the study of the complexing ability of the ligands to the selected metal ions. An electrochemical cell comprising three electrodes was employed: thin film mercury coated carbon microelectrode was used as the working electrode, a Platinum wire as the auxiliary electrode, and a Ag/AgCl as the reference electrode.

CV has been used and proven to offer a convenient route towards the determination of metal-ligand complex stability constants in aqueous media*. The values of the logarithms of the metal-ligand formation constants obtained by this technique, when compared with other widely used aminopolycarboxylic acids (APCAs), show better complexing ability of the ligands with the transition metal ions. When the two ligands are compared, IGS showed greater affinity towards the selected transition metal ions. This is due to the fact that, in aqueous media, as the side chain ligators decrease, the stabilization energy of the complex increases. The formation stability constants were determined by plotting the change in the reduction potential (ΔE) against solution pH. A process making use of a modification of lingane equation was used.

---

*A.M. Crouch, L. E. Khotseng, M. Polhuis, D. R. Williams, *Analytical Chemical Acta,* 2001, **448,** 231-237

# Opsomming

Twee nuwe potensieel bio-afbreekbare amienpolikarboksielsuurligande, iminobiglutaarsuur-tetranatriumsout (IBG-4Na) en iminoglutaarsuksiensuur-tetranatriumsout (IGS-4Na), was vervaardig met redelike goeie opbrengs en suiwerheid. Die kommersïeel onverkrygbare voorloper van die twee ligande, etiel-ß-aminoglutaraat, was berei met hoë obrengs en suiwerheid, en was saam met die twee ligande ten volle geïdentifiseer deur middel van smeltpunt bepalings en verskeie spektrometriese tegnieke ($^1$H-KMR, $^{13}$C-KMR, MS en IR.).

Vir die eerste keer is 'n elektrochemiese studie uitgevoer op die komplekse van hierdie ligande met selektiewe oorgangsmetaalione ($Zn^{2+}$, $Cu^{2+}$, en $Cd^{2+}$). 'n Elektrochemiese tegniek, sikliese voltametrie (SV), is gebruik om die komplekseringsvermoë van die ligande ten opsigte van die geselekteeerdr metaalione te bestudeer. 'n Elektrochemiese sel wat bestaan uit drie elektrodes is gebruik: 'n Dunlaag kwikelektrode bedek met koolstof is gebruik as die werkselektrode, 'n platinumdraad as die bykomende elektrode en 'n Ag/AgCl elektrode as die verwysingselektrode.

SV is voorheen gebruik en bewys as 'n gerieflike metode vir die bepaling van metaalligandkomplekssstabiliteitskonstantes in waterige media*. Die waardes van die logaritmes van die metaalligandvormingskonstantes wat verkry word deur hierdie tegniek, soos vergelyk met ander algemeen gebruikte amienpolikarboksielsure (APKSe), vertoon beter komplekseringsvermoë met die ligande deur middel van die oorgangsmetaalione. Wanneer die twee ligande met mekaar vergelyk word, het IGS-4Na groter affiniteit gehad vir die oorgangsmetaalione. Dit is as gevolg van die feit dat die stabiliteitsenergie van die kompleks in waterige media verminder word soos wat die sykettings van die ligande toeneem. Die vormingstabilitietskonstantes was bepaal deur 'n varandering in reduksie potensiaal (ΔE) teenoor die pH van die oplossings te plot. Die grafieke is verkry deur 'n aanpassing van die Lingnane-vergelyking te gebruik.

---

* A.M. Crouch, L. E. Khotseng, M. Polhuis, D. R. Williams, *Analytical Chemical Acta,* 2001, **448,** 231-237

# Dedication

**To my Mother, Father and Siblings**

# Acknowledgements

I would like to thank the following people and organizations for contributing to the success of my research work:

- **Prof. A.M. Crouch**, my promoter, for his academic help, patience, encouragement and financial support.
- **Dr. M.W. Bredenkamp**, my co-supervisor, for his academic help and encouragement.
- **My parents, brothers** and **sisters** for being there always to support me morally and financially during the course of this programme.
- Members of the **Eri-Maties Christian Fellowship** for their support in prayers.
- **Tedros Goje**, for being a good colleague and for his unfailing friendship.
- **Yared Tesay** and **Isaac Hidru** for their moral support and for being good flat-mates.
- **The Eritrean Government** for sponsoring my study.
- **The International office** of the University of Stellenbosch for their financial support.
- **Leon** and **Estella**, my colleagues in the organic laboratory, for being supportive to me.
- **All my colleagues,** in the analytical research group, for always creating a conducive working environment in the laboratory.
- **Elsa and Jean,** for working diligently in running my NMR spectra.
- **Adriana** for translating my abstract into Afrikaans

# List of Abbreviations and Symbols

| | |
|---|---|
| A | -Amps |
| AAS | -Atomic Absorption Spectrometry |
| AdsV | -Adsorptive Stripping Voltammetry |
| APCAs | -Amino Poly Carboxylic Acids |
| ASDA | -Asparaginic acid Diacetic Acid |
| BAS | -Bio analytical system |
| C | -Concentration |
| CV | -Cyclic Voltammetry |
| $^{13}$C-NMR | -$^{13}$C nuclear magnetic resonance |
| D | -Diffusion coefficient |
| DME | -Dropping mercury electrode |
| $D_2O$ | -Deuterated water |
| DPASV | -Differential pulse anodic stripping voltammetry |
| DTPA | -Diethylenetriaminepentaacetic acid |
| DTPMP | -Diethylenetriaminepentamethylenephosphonic acid |
| E | -Potential |
| $E^o$ | -Standard potential |

| | |
|---|---|
| $\Delta E_p$ | -Separation between peak potentials |
| $E_{pa}$ | -Anodic peak potential |
| $E_{pc}$ | -Cathodic peak potential |
| EDTA | -Ethylenediaminetetraacetic acid |
| EDDHA | -Ethylenediaminedi(o-hydroxyphenyl)acetic acid |
| EDDS | -Ethylenediaminedisuccinic acid |
| EDTMP | -Diethylenetriaminepentamethylenephosphonic acid |
| ETAAS | -Electro-thermal atomic absorption spectrometry |
| F | -Faraday's Constant |
| HEDTA | -Hydroxyethylethylenediaminetriacetic acid |
| HMDE | -Hanging mercury drop electrode |
| HMP | -Hexamethaphosphate |
| $^1$H-NMR | -$^1$H nuclear magnetic resonance |
| $i_p$ | -Peak potential |
| ICP-AES | -Inductively coupled plasma –atomic emmision spectrometry |
| ICP-MS | -Inductively coupled plasma -mass spectrometry |
| IDG | -Iminodiglutaric acid |
| IGS | -Iminoglutaricsuccinic acid |
| IDG-4Na | -Iminodiglutaric acid tetra sodium salt |

| | |
|---|---|
| IGS.4Na | -Iminoglutaricsuccinic acid tetra sodium salt |
| IR | -Infrared |
| LH | -Protonated ligand |
| $\log K_{1,2,3}$ | -Stepwise logarithmic formation constants |
| $\Sigma \log K_f$ | -Summation of logarithmic formation constants |
| MFE | -Mercury film electrode |
| MGDA | -Methylglycinediacetic acid |
| ML | -Metal-ligand complex |
| MS | -Mass Spectrometry |
| n | -Number of electrons |
| NTA | -Nitriloacetic acid |
| NTMP | -Nitrilotrimethylenephosphonic acid |
| OECD | -Organization for Economic and Cooperation Development |
| SCE | -Saturated calomel electrode |
| SMDE | -Static mercury drop electrode |
| SME | -Streaming mercury electrode |
| $\delta$ | -NMR chemical shift in parts per million (ppm) |
| T | -Temprature in Kelvin |
| TMS | -Trimethylsilane |

| | |
|---|---|
| TPP | -Tripolyphosphate |
| V | -Volt |
| υ | -Scan rate |

# List of Figures

# List of Tables

# Table of Contents

# Chapter One

## Introduction

# 1 Introduction

## 1.1 Biodegradability and Environmental Risk

Biodegradability* is a key property in the environmental hazard and risk assessment of organic chemicals.[1] A biodegradable chelant is one which complies with the OECD criteria. The OECD criteria states that "60% of the compound must biodegrade within 28 days and 10% within 10 days" [2]

Due to the fact that chelants are mostly employed in water based applications and are disposed off via sewage treatment plants from where they are released into the environment, close attention has been given to the chelants with respect to their environmental behaviour and risk. From the number of concerns that were raised it turns out that the potential of chelants to mobilize heavy metals from sediments or soils and their subsequent transport into drinking water was the most critical point. Due to their strong complexing ability and persistence in the environment most chelants were identified as environmentally problematic. Hence one of the most important elements in the risk assessment of organic chemicals or chelants (e.g. APCAs) is their ability to (bio)degrade during sewage treatment and in the natural environment. [3]

---

* Biodegradability is the metabolism of organic chemicals as sources of carbon and energy by microorganisms to form microbal mass and sample energy products, such as methane and carbon-dioxide.

Despite their tremendous industrial and domestic applications, most chelants and their complexes with heavy metals are chemically and biologically stable and hence cause environmental risk. The cause of the relative biological stability of ethylenediamine-based compounds (e.g. EDTA, DTPA) has not yet successfully explained. Some data suggest that complexes with high stability constants are less or not at all degradable.[4, 5] However, some authors even approved biodegradability of very stable $Fe^{III}$ complexes hence it seems that there is no clear relationship between the stability constant and degradability. [6, 7, 8] The rates of photodegradation of the iron(III) chelates apparently increase in the order NTA<EDTA<DTPA. [4]

Only compounds containing one nitrogen atom in the molecule (e.g. NTA) have shown biological degradability. A relationship exists between the chemical structure and biodegradability of organic substances. [9] The relationship between the structure of complexing agents and their biodegradability remains to be answered. However, a primary amine seems to be a prerequisite for biodegradability

With increasing concern for the welfare of the environment, it has become necessary to design new potentially biodegradable ligands and replace some, if not all, of the non-biodegradable ligands, currently preferred in industrial processes, as they and their complexes with toxic heavy metal ions are not readily biodegradable and thus tend to accumulate in the biosphere.[10]

## 1.2. Objectives of the study

- To synthesis new "biodegradable" ligands- iminodiglutaric acid (IDG) and iminoglutaricsuccinic acid (IGS)

- To determine the physico-chemical properties of selected metal complexes of iminodiglutaric acid (IDG) and iminoglutaricSuccinic acid (IGS), using cyclic voltammetry. These are novel ligands and their equilibrium characteristics need to be known for speciation prediction

## 1.3. Heavy Metals

### 1.3.1 Occurrence

Metals in the environment are due to both natural (e.g. ore deposits and volcanoes) and anthropogenic sources (e.g. coal burning, metallurgical industry and waste incineration.[11]). It has been pointed out that some metal emissions of anthropogenic origin exceed the natural sources by large factors.[12] Industrialization and domestic activities have accelerated biogeochemical cycles of a large number of elements, including heavy metals. This has contributed to the increasing deposition of heavy metals in natural ecosystems. Moreover, heavy metals occur in petroleum products and therefore represent a serious problem for the environment and living organisms.[13, 14]

### 1.3.2 Toxicity

The toxicity of metals depends not only on their total concentration, but also on their mobility and reactivity with other components of the ecosystem. The reactivity or mobility of heavy metals in soils or sediments, and thus their toxic potential, depends upon speciation and which chemical and physical processes different phases are subject to.[15] Toxicity is directly related to its reactivity with living matter. Living organisms are exposed to them through respiration, skin contact and consumption.

Heavy metals may be amongst the most harmful pollutants. Among these are Cd and Pb ions that are generally toxic, even at a very low level, and potentially toxic metals such as

Cu and Zn ions.[11] At trace levels, most of metals are essential to life (trace elements). Some of the biochemical essential elements are Cu, Zn, Co, Ni, V, Se, Fe and Mn, though become progressively toxic above certain levels. Some of these metals, Ni, Cr, Cu and Se are known to display carcinogenic effects due to their interaction with nucleic acids. For instance, $Cu^{2+}$ ions are essential nutrients, but when humans are exposed to Cu levels of above 1.3 mg/l for short periods of time, stomach and intestinal problems occur. Long-term exposure to $Cu^{2+}$ leads to kidney and liver damage.[16]

Moreover, pollution of ground water, soil and air with toxic heavy metals like mercury, cadmium, lead, etc. poses a serious health risk. For instance, inhalation of fumes or dusts containing lead compounds (lead halide aerosol emitted by automobile) can enter the lungs and be absorbed directly into the blood stream. The main sources of soil and ground water pollution are improper waste dumping, agricultural chemicals, and industrial effluents, [17, 18] which are all due to anthropogenic activity. If the environment is severely polluted by heavy metals, it is necessary to prevent pollution spreading and to restore the contaminated environment to previous conditions as soon as possible. In particular, the rapid diffusion of heavy metals as environmental contaminants has called for attention to their determination at trace and ultratrace levels and especially to their speciation.

### 1.3.3 Metal Detection Techniques

Sensitive, fast, reproducible, simple and accurate analytical methods are required for the determination of trace elements in geological, biological and environmental samples. Accordingly, there have been extensive efforts to enhance the sensitivity and lower the detection limits of instrumental methods of analysis. There exists a need for rapid and wide scale monitoring of heavy metals in the environment. Simple, sensitive sensors that can measure multiple elements simultaneously would be of great significance for wide scale monitoring.

Among the various detection techniques for metal analysis, electro-thermal atomic absorption spectrometry and inductively coupled plasma mass spectrometry ET-AAS and ICP-MS are the most attractive ones because of their high sensitivities and low detection limits [19, 20, 21] which in the case of ICP-MS is augmented furthermore by its capability of isotope ratio and multi-element measurements.[19] Yet, the practical applicability of the ICP-MS technique is frequently restricted by spectral and non-spectral interferences because of its inherently low tolerance limit to sample constituents present in biological or environmental matrices, including high concentrations of easily ionised elements, salts, mineral acids and organic solvents. [20] However, the major limitations of ICP-MS at this time may be its cost, the need for highly trained personnel for proper operation and that the technique is not available for routine use in many places. In addition, the current status of ICP-MS software makes its automation problematic. ET-AAS instrumentation, in contrast, is available in most clinical and analytical laboratories

and it is sufficiently sensitive to be directly applied for the routine determination of most metallic elements at $\mu g\ l^{-1}$ levels.[19]

As opposed to ICP-MS, ETAAS may tolerate samples with different morphology and chemical composition such as brines, sludges, slurries, and highly viscous samples. [19] However, complex samples cannot be directly processed with ET-AAS as they pose severe matrix interferences.

The direct determination of extremely low concentrations of the required trace elements by modern atomic spectroscopic methods, such as atomic absorption spectrometry (AAS) and inductively coupled plasma atomic emission spectrometry (ICP-AES) is often difficult [19]. The limitations are not only associated with the insufficient sensitivity of these techniques but also with matrix interference. For this reason, the preliminary separation and pre-concentration of trace elements from the matrix is often required (e.g. liquid-liquid extraction, [22] solid-phase extraction, [23] co-precipitation, [24] ion-exchange [25]evaporation [26] and electrochemical deposition [27])

Voltammetric methods are very attractive for determining heavy metals at trace levels. Pure liquid mercury or liquid mercury amalgams are superior as electrode materials in voltammetry for analytical purposes.[28, 29, 30] This is mainly due to the high overvoltage for hydrogen, which makes possible a wide working potential range for the electrode. The most popular one, for environmental samples, is anodic stripping voltammetry (at a

mercury film electrode[31]). This technique is very sensitive for many metals, it offers the capability of low cost multi-element analysis and it is suitable for automation. In particular, it is favorable for the determination of cadmium, copper, lead and zinc.[32, 33] However, for many metal ions (e.g. Pb, Cd, Cu, and Zn); DPASV (differential pulse anodic stripping voltammetry) at a mercury film electrode is also used. For DPASV, the pre-concentration step involves reduction of the metal ions followed by amalgamation with the mercury film surface. [34] Also, AdsV (adsorptive stripping voltammetry) is known to give an excellent sensitivity for a variety of trace metals at a mercury electrode (film or drop). [35] This method involves complexation of trace metals with metal-specific ligands and adsorbing the resulting complex onto the mercury surface (film or drop). The adsorbed metal complex is electrochemically removed by scanning the electrode potential, usually in a reductive direction. Since this is a surface technique, it is suitable for determining ultra-trace levels ($10^{-10}$ M) of metals in solutions. [36]

Stripping voltammetric techniques may be certainly a good alternative to spectroscopy, since it allows the carrying out of a multi-component determination at concentration level down to the fractional parts per billion (sub-ppb) and it does not need too expensive equipment. [37] Among its spectroscopic competitors only flameless atomic absorption has nearly the same sensitivity, but at much higher cost. The remarkable sensitivity of stripping voltammetry is attributed to the unique coupling of an *in situ* pre-concentration step with an advanced voltammetric measurement of the accumulated analyte. [38] Stripping instruments are small in size, have very low power demand and require no special installation such as cooling or ventilation. None of the other techniques for trace

metal detection (quantification) can compete with stripping analysis on the basis of sensitivity per money invested.

There has, however, been a growing concern about the general use of mercury because of its toxicity. This includes the use of pure mercury as an electrode material in voltammetry. Even for laboratory use, restrictions are expected to appear in the future. Therefore, it is of great interest to find new alternative electrode materials for use in voltammetry.[34] Numerous papers have been published dealing with alternative electrodes, but all these electrodes have limited analytical value because they cannot operate at negative potentials because of their low hydrogen overpotential. This is a great drawback since important metals like zinc, nickel and cobalt have half-wave potentials at more negative values, and therefore cannot be detected by the use of these electrodes.

## 1.4 Chelants

In an aqueous environment free metal ions can catalyze many unwanted chemical reactions such as the formation of Mg and Ca precipitations during washing, the decay of bleaching agents in pulp and paper production processes or in detergents, or fats and oils becoming rancid. Therefore, it is often necessary to control the availability and accessibility of free metal ions in chemical production processes as well as in products. This can be achieved by "capturing" the positively charged di- and tri-valent metal ions

with negatively charged compounds.[3] These electron-donating compounds are the chelants of the different classes, which have tremendous application in industry.

A chelant (chelating agent) is a polydentate ligand*, *i.e.* it can bind to the metal ion with more than one atom, forming a ring. The word chelant was derived from the Greek *chele*, meaning a lobster's claw [39] describing the way in which the ligand binds by wrapping itself around the metal ion. The chelating agent may be bidentate, tridentate, tetradentate, with the number of its "teeth" corresponding to the number of donor atoms in the molecule that simultaneously complex the metal ion. Monodentate molecules, having only one donor atom, such as water, ammonia, *etc.*, are considered complexing agents but not chelants. [40] Thus the term chelate is reserved for a complex formed between a metal ion and multidentate legand, which forms ring(s) during complexation with the chelated metal ions at the center of the complex.

### 1.4.1 Classes of Chelants

Chelating agents may be either organic or inorganic compounds, but the number of inorganic chelants is small. The best-known inorganic chelants are polyphosphates, also known as "glassy phosphates" such as tripolyphosphate (TPP) and hexametaphosphates. Polyphosphates tend to be less expensive than organic chelants, but they are

* Ligand is an atom or molecule or radical or ion that forms a complex around a central atom

hydrolytically unstable at high temperatures and pH levels. [40] The three commonly used organic industrial chelating agents (aminopolycarboxylic acids, polycarboxylic acids, and phosphonic acids) possess many of the complexing properties of the inorganic polyphosphates, but, unlike the polyphosphates, these chelating agents are stable in water under high temperatures and pH.

| No. | Chelating agents | Class | Uses | Pros and Cons |
|---|---|---|---|---|
| 1 | **Aminopolycarboxylic acids (APCAs)**<br>e.g. EDTA, DTPA, NTA, EDDHA… | Organic | Removal of hardness salts; boiler cleaning; brewery; power plant and dairy applications; metal cleaning; rust removal; gas conditioning; (e.g. sulphur removal); petroleum drilling fluids; wood pulp processing | Are stable at high temperature and pH; strong affinity for metals, somewhat expensive; predominantly not biodegradable |
| 2 | **Phosphonic acids**<br>e.g. EDTMP, DTPMP, NTMP, | Organic | Water treatment,<br>e.g. scale and corrosion inhibition in:<br>- cooling towers;<br>- wood pulp processing;<br>- metal plating<br>- polymer processing | Stable over a wide range of temp. and pH levels; Are expensive |
| 3 | **Polycarboxylic acids**<br>e.g. gluconates, citrates, polyacrylates, polyaspartates | Organic | Processing at high pH levels;<br>Hardness-ion sequestration | Are inexpensive, but weak chelants |
| 4 | **Polyphosphates**<br>e.g. TPP, and HMP | Inorganic | Water-treatment system; cleaning applications; cosmetics | Unstable at high temp and pH levels, Are inexpensive |

**Table 1.** Classes of chelating agents

The first complexing agents employed in modern detergents were di- and triphosphates. However, it was soon found that these contribute to the eutrophication [3](an excessive growth of algae) of lakes and rivers. During the search for substitutes, NTA was proposed as an alternative detergent builder and NTA-containing detergents were first marketed in Sweden in 1967.[41] Thus, many phosphates have been replaced by aminopolycarboxylates.

Hence due to the reason mentioned above, APCAs (also known as "complexones"[4,40,]) are the most important group of organic compounds used nearly in all industrial applications. Moreover these chelants, their stability over broad pH and temperature ranges, and their strong affinity for metals makes them more attractive for metal ion sequestering applications. [40] APCAs contain several carboxylate groups linked to one or several nitrogen atoms (Fig. 1) and they are able to "cage" (complex) the metal ion by forming one or more stable heteroatomic rings onto it. [3] This ring formation leads to the higher stability of the chelates as compared to the metal-ligand complex in which no such rings are present, a phenomenon, which is called the "chelate effect". [4] There are a number of natural (EDDS, Rizobactin, Nicotinamic, Avenic....) and synthetic (NTA, EDTA, DTPA, IDG, IGS, HEDTA, EDDHA, ASDA *etc*) APCAs (Fig. 1).

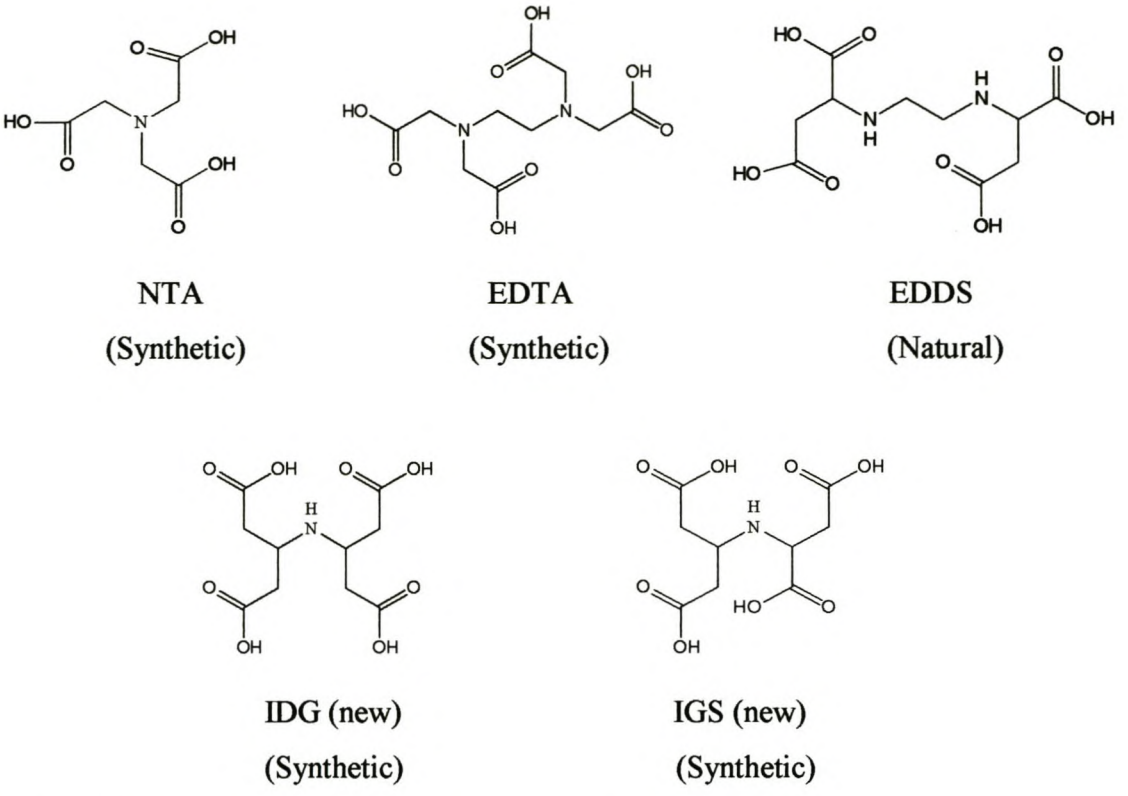

NTA (Synthetic) EDTA (Synthetic) EDDS (Natural)

IDG (new) (Synthetic) IGS (new) (Synthetic)

**Figure.1.** Some examples of natural and synthetic APCAs

The last two ligands (IDG and IDS), in their tetra-sodium salt forms, were synthesized in our laboratory.

### 1.4.2 Synthesis of APCAs

APCAs are compounds that contain several carboxylate groups bound to one ( NTA, IDS, IDG, IGS *etc*) or more ( EDTA, EDDS, EDDM, *etc*) nitrogen atom (Fig 1). Hence they must be derived from the amino acid, glycine. [3, 4] The first APCA, NTA, was synthesised in 1862 by Heintz [3] and only 70 years, later, 1935, the APCA presently used in the largest

amounts, EDTA, was synthesised by I.G. Farbenindustrie in Germany. The synthesis of NTA was based on the reaction of monochloroacetic acid in an ammonical solution. Again, the synthesis of EDTA was based on monochloroacetic acid reacting with ethylenediamine in the presence of sodium hydroxide. Alternatively, EDTA is synthesised from ethylenediamine reacting with sodium cyanide and formaldehyde in the presence of sodium hydroxide. [4] Depending on the amine employed, also other APCAs, for instance PDTA, can be produced by this type of reaction. IDS, an environmentally friendly ligand in its sodium salt form, is synthesised by treating maleic anhydride with water, ammonia and sodium hydroxide.

Lately, reports have shown the synthesis of many APCAs, namely β-ADA, SDA and MGDA. They are derived from amino acids by substituting the amino group with two acetyl groups.

Until some years ago APCAs were thought to be a typical anthropogenic class of compounds but the number of reports on naturally occurring APCAs, for instance EDDS, produced by microorganism is increasing. The chiral APCA, S,S-EDDS, produced by an actinomycete appear to have considerable commercial potential because it has metal-complexing properties similar to EDTA.[3]

### 1.4.3 Applications of Chelants

Metal ions are a problem in virtually all aqueous processes. A common problem is the scale formed by precipitation of alkaline earth and of heavy metal salts, which blocks pipes and valves. Transition (heavy) metal ions also catalysed unwanted degradation reactions, rendering formulations useless. [42] The most effective solution is to use chelants to mask the metal ions, thus keeping them in solution or preventing them from catalyzing unwanted reactions.

Thus chelating agents are critical allies in the "war" against metal-ion-induced equipment and process problems. [40] In this respect their function is fourfold: [4] (i) to prevent the formation of metal precipitates, (ii) to hinder metal ion catalysis of unwanted chemical reactions, (iii) to remove metal ions from systems, and (iv) to make metal ions more available by keeping them in solution.

Phosphate chelants, for example, are used as scale and corrosion inhibitors in cooling towers. [40] In industrial cleaning agents, NTA, ETDA, and recently also MGDA, are also used to prevent precipitation of calcium, magnesium and heavy metal salts. [43, 44, 45] Detergents, in addition to active washing ingredients, contain a large proportion of metal-complexing agents to inhibit the formation of insoluble $Ca^{2+}$ and $Mg^{2+}$ salts, and thus prevent the deposition of scale on both textile fibres and washing machine parts.

In wood pulp processing, detergent formulations of metal ions [44] ($Fe^{3+}$, $Cu^{2+}$, and $Zn^{2+}$, $Mn^{2+}$) can catalyze the degradation of oxidative and reactive bleaching chemicals, such as hydrogen peroxide and sodium hydrogensulphate. [40] Chelants can be added directly to bleach liquor to control metal ion in situ, or chelant washes can be done as a bleaching pre-treatment, to remove harmful metal ions before bleach comes in contact with wood pulp. Chelating agents (APCAs) are also used as additives for pharmaceuticals, cosmetics and food to prevent transformation of the ingredients or rancidity due to metal-catalysed reactions [43, 46] Moreover, multidentate chelating agents, because they form water soluble complexes with many radionuclides, can be used in the nuclear industry for decontamination of reactors which consequently removes the metal ions from the reactor.

The metal availability in soils can be attained by metal chelants. Especially APCA chelators are employed in fertilisers to supply plants with trace metals such as iron, copper, zinc and manganese. Most commonly, the Fe(III) chelates of EDTA, HEDTA, DTPA, EDDHA and ethylenediaminedi(2-hydroxy-4-methylphenyl)acetic acid and the Cu(II), Zn(II) and Mn(II) chelates of EDTA are present in fertilisers.[47] Their presence improves plant nutrition. [48]

Chelated metals can also offer chemical properties that can be used to advantage by changing the redox properties of certain metal ions in the process stream. In gas conditioning, for instance, iron chelates of APCAs are frequently used to treat sulfides. In this case, the iron chelate is formed, while the sulphide is oxidized to elemental sulphur for removal. [40]

## 1.5 References


1. H. Loonen, F. Lindgren, B. Hansen, W. Karcher, J. Niemela, K. Hiromatus, M. Takatsuki, W. Peijnenburg, E. Rorije, J. Struijs, *Environmental Toxicology and Chemistry*, 1999, **18**, 1763-1768
2. W.P. Jones, D.R. Williams, *Applied Radiation and Isotopes,* 2001, **54**, 587-593
3. T. Egli, *Journal of Bioscience and Bioengineering*, 2001, **92**, 89-97
4. M. Bucheli-Witschel, T. Egli, *FEMS Microbiology Reviews,* 2001, **25**, 69-106
5. L. Henneken, B. Nörtemann, D.C. Hempel, *Appl. Microbiol. Biotechnol.*, 1995, **44**, 190–197
6. R.T Belly, J.J. Lauff and C.T. Goodhue, *Appl. Microbiol.* 1975, **29**, 787–794
7. J.J. Lauf, D.B. Steele, L.A. Coogan, J.M. Breitfeller, *Appl. Environ. Microbiol.* 1990, **56**, 3346–3353
8. M. Witschel, S. Nagel, T. Egli, *J. Bacteriol.*, 1997, **179**, 6937–6943
9. P. Pitter, and J. Chudoba, *Biodegradability of Organic Substances in the Aquatic Environment*, 1990, CRC Press, Boca Raton
10. A.M. Crouch, L.E. Khotseng, M. Polhuis, D.R. Williams, *Analytical Chemical Acta,* 2001, **448**, 231-237
11. H.W. Nurnberg, *Anal. Chim. Acta.*, 1984, **164**, 1-24
12. U.R. Ayres, *Resour. Conserv. Recycling,* 1997, **21**, 145–173
13. M. Mullen, D. Wolf, F. Ferris, T. Beveridge, C. Flemming, G. Bailey, *Appl*

*Environ. Microbiol.*, 1989, **55**, 3143–3149

14. G. Gadd, A. Griffiths, *Microb. Ecol.*, 1978, **4**, 303–317.

15. P. Micaela, E. C. Malcolm, *Environment International,* 2002, **28**, 433-449

16. R. Molinari, S. Gallo, P. Argurio, *Water Research,* 2004, **38**, 593-600

17. J. Chen, M. Wey, Y. Lin, *Chemosphere,* 1998, **37**, 2617–2625

18. O. Abollino, M. Aceto, M. Malandrino, E. Mentasti, C. Sarzanini, R. Barberis, *Environ. Pollut.*, 2002, **119**, 177–193

19. J. L. Burguera, M. Burguera, *Spectrochim. Acta,* 2001, **56**(B), 1801

20. K. Benkhedda, H.G. Infante, F. Adams, E. Ivanova. *Trends Anal. Chem.*, 2002, **21**, 332

21. E.V. Alonso, A.G. Torres, J. Mc. Pavón, *Talanta*, 2001, **55**, 219

22. C.W. Mcleod, A. Otsuki, K. Okamato, H. Haraguehi, K. Fuwa, *Analyst*, 1981, **106**, 419

23. G. Kudrgavstev, P. Nasterenko, V. Ivanov, A. Savitchev, N. Smirnova, *Talanta*, 1991, **38**, 675

24. C. Frigge, E. Jackwerth, *Anal. Chim. Acta,* 1991, **242**, 99

25. J. Dumont, M. Cote, J. Hubert, *Appl. Spectrosc.*, 1989, **43,** 1132

26. J. R. Castillo, J. M. Mir, M.E. Garcia-Ruiz, C. Bendicho, *Anal. Chem.*, 1990, **338,** 721

27. G.E. Batley, J. P. Matousek, *Anal. Chem.*, 1980, **52**, 1570

28. J. Wang, *Analytical Electrochemistry*, 2nd Edition, Wiley-VCH, New York, 2000.

29. Ø. Mikkelsen, K. H. Schrøder, *Electroanalysis,* 1999, **11**, 401

30. Ø. Mikkelsen, K.H. Schrøder, *Anal. Lett.* 2000,**33**, p. 3253

31. G. Scarponi, G. Capodaglio, P. Cescon, 1982, **135**, 263-276

32. W. Martinotti, G. Queirazza, A. Guarinoni, G. Mori, *Anal. Chim. Acta*, 1995, 305, 183–191

33. O.A. Farghaly, A.M.M. Ali, M.A. Ghandour, *J. Anal. Chem.*, 1999, **8**, 70–83.

34. L. Mart, H. W. Nurnberg, P. Valenta, Fresenius, *Anal. Chem.*, 1980, **300**, 350

35. A.M. Paneli, A. Voulgaropoulos, *Electroanalysis*, 1993, **5**, 355-373

36. O.A. Farghaly, *J. Microchemical*, 2003, 75, 119-131

37. L. Clinio, T. Giancarlo, *J. Microchemical,* 2003, **75**, 233-240

38. J. Wang, M. Czae, J. Lu, M. Vuki, *J. Microchemical*, 1999, **62**, 121-127

39. S.M.I. Hetland, B. Radzuk, Y. Thomassen, *Anal. Sci.*, 1991, **7**, 1029

40. M. Conway, S. Holoman, L. Jones, R. Leenhouts, G. Williamson, *Chemical Engineering,* 1999, 86-90

41. R.L. Anderson, E.B. Bishop, R.L. Campbell, *Crit. Rev. Toxicol.*, 1985, **15**, 1–102

42. J.R. Duffield, F. Marsicano, M. Waters, D.R, Williams, *Polyhedron*, 1991, 10, 1113-1120

43. K. Wolf, P.A. Gilbert, EDTA-ethylenediaminetetraacetic acid. In: The Handbook of Environmental Chemistry, 1992, 3 (Hutzinger, O., Ed.) 241–259. Springer, Berlin

44. R. Klopp, B. Pätsch, *Wasser Boden,* 1994, **8**, 32–37

45. F. Sacher, E. Lochow, H.J. Brauch, *Vom Wasser* 1998, **90**, 31–41

46. F. Zhao, J. Yang, C. Schöneich, *Pharmacol. Res.*, 1996, 931–938

47. M.S.M.R. Deacon, L.G.M.T. Tuinstra, *J. Chromatogr.*, 1994, **659**, 349–357

48. A. Wallace, G.A. Wallace, J. W. Cha, *J. Plant Nutr.*, 1992, **15**, 1589–1598

# Chapter Two

## Synthesis of Biodegradable Ligands- Iminodiglutaric Acid and Iminoglutaricsuccinic Acid

# 2 Synthesis of New Biodegradable Ligands-IDG and IGS

## 2.1 General

Reaction scheme 2 shows the general synthetic route for both IDG and IGS. Both ligands were prepared in a similar way. The only difference was in the reagents used. In the case of IDG, ethyl β-Aminoglutarate (diethylaminoglutarate) was reacted with diethyl glutaconate. However, diethylmaleate was used instead of diethyl glutaconate in the IGS synthesis. Since diethylaminoglutarate is not commercially available, its hydrochloride crystal form was synthesised according to literature method developed by W.A. Swarts *et al.*[1] The product was characterized using various spectroscopic techniques. (NMR, IR and MS)

## 2.2 Experimental Approaches

### 2.2.1 Synthesis of Ethyl β-Aminoglutarate

Reaction scheme 1 shows how ethyl β-aminoglutarate can be synthesised in three possible ways. In our study the second method was employed.

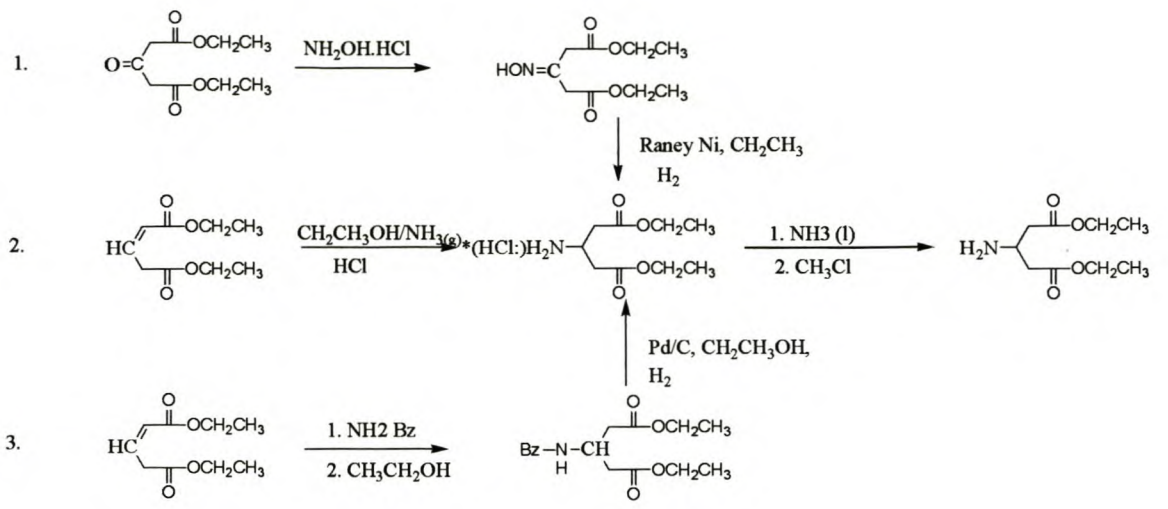


*The HCl is covalently bonded to the N-atom only when method 2 is employed

**Reaction Scheme 1:** Three possible synthetic routes for ethyl β-aminoglutarate.

Absolute ethanol was dried by distillation off $Mg(OEt)_3$. Dry ammonia gas was bubbled through the dry ethanol (150 ml), in a three-necked round-bottomed flask, until it was saturated and diethyl glutaconate (15 gm) was added in one portion. The temperature was maintained at 50-55 °C while ammonia was continually passed through the solution for 36 hours.

The removal of ammonia and ethanol, after 36 hours of reaction, in *vacuo,* afforded a slightly green-yellowish oil, which was then taken up in 100 ml of dry ether. Some undissolved material remained; which was removed from the solution by filitration and washed with 2x50 ml portions of ether. The washings were combined with the ethereal solution and upon addition of dry hydrogen chloride (HCl gas was synthesises according to the procedure.

**Reaction scheme 2**: The general synthetic route for IDG and IGS

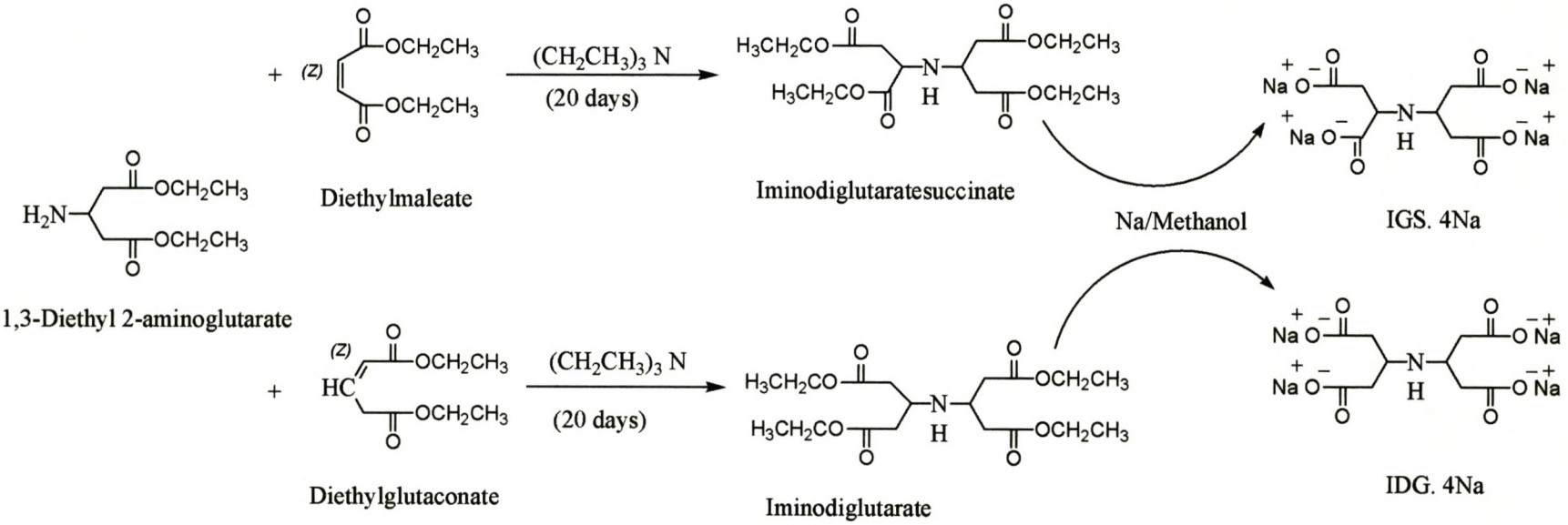

described in 2.2.1.1) oil was separated which soon crystallized. The white crystals were collected by simple filtration. Dissolution in chloroform followed by re-crystallization (the solution was left over night for crystal growth) by addition of ether afforded a total of 13.5 gm (70%) of ethyl β-aminoglutarate hydrochloride (white crystal), m.p. 84°C (lit[1]. m.p. 83.5-84.5°)

The product was characterised using various spectroscopic techniques ($^{1}$H-NMR, $^{13}$C-NMR, IR, and MS).

### 2.2.1.1 Production of Dry Hydrogen Chloride

Hydrogen chloride gas is liberated when sulphuric acid is reacted with sodium chloride according to the following reaction:

$$H_2SO_4 + 2NaCl \longrightarrow Na_2SO_4 + 2HCl\uparrow$$

Briefly the procedure is as follows:

A quarter of mole of analytical reagent sodium chloride was placed in a two-necked round-bottomed flask. Concentrated sulphuric acid (98%) is added carefully, drop-wise, to the salt, from a dropping funnel. The hydrogen chloride gas produced from the two-

necked round-bottomed flask (according to the above reaction) was directly bubbled into the ethereal solution. The flow rate of the gas is carefully monitored by a bubble flow meter.

#### 2.2.1.1.1 Removal of HCl

The white crystal like ethyl β-aminoglutarate hydrochloride is dissolved in a minimum amount of water, which is then basified with ammonia to a pH of 11. Ethyl β-aminoglutarate is then extracted with chloroform (25 ml x4). The extract is dried overnight with anhydrous magnesium sulphate. After filtering the solution the chloroform is evaporated to yield ethyl β-aminoglutarate as colourless oil. Product was characterised using various spectroscopic techniques ($^{1}$H-NMR, $^{13}$C-NMR, IR, and MS).

### 2.2.2 Synthesis of Iminodiglutaric acid tetra sodium salt (IDG 4Na)

The method reported by A.K. Saxena *et al.*[2] was adopted for the synthesis of the symmetric compound iminodiglutarate (the ester form of iminodiglutaric acid). Thereafter, the ester was hydrolyzed to get a new potentially biodegradable ligand, iminodiglutaric acid tetra-sodium salt (IDG 4Na). The experimental procedure is, briefly, as follows:

A mixture of 9 g (48.4 mmol) of ethyl β-aminoglutarate (synthesised by the above method), 9.82 g (48.4 mmol) of diethyl glutaconate and 1.42 ml of triethylamine is placed in a hermetically sealed round-bottomed flask at 32°C for 20 days. The reaction mixture (after 20 days) is extracted with 37 % hydrochloric acid solution (4 x 20 ml). The extract is basified with excess ammonia solution (very vigorous exothermic reaction). The separated oil is extracted with chloroform (4 x 20 ml), which is then dried with magnesium sulphate (for over night) and roter-evaporated to give IDG in its ester form. Product was characterised using NMR spectroscopic techniques.

The four ethyl groups in the above product were removed by the following hydrolysis reaction:

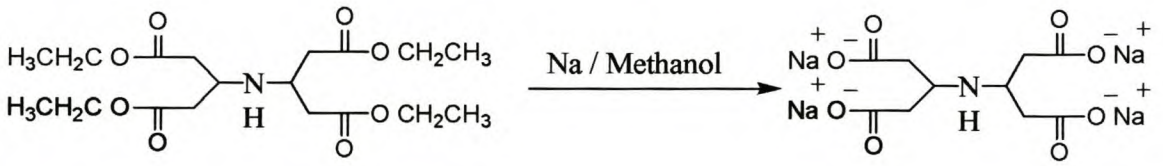


**Figure 2** Hydrolysis of Iminodiglutarate

In a two necked round bottomed flask, provided with a small condenser and 40 ml of methanol, 8 g of sodium was dropped. The mixture was heated until all the sodium had dissolved. After cooling the reaction mixture, 2 g of the ester and 2 ml of water is added. Thereafter, the sodium salt of the acid is rapidly precipitated. The solid, IDG.4Na, is filtered off and washed with a little methanol and dried. Product was analysed spectroscopically.

### 2.2.3 Synthesis of Iminoglutaricsuccinic acid tetra sodium salt (IGS. 4Na)

In an identical experimental approach, as for IDG, a new potentially biodegradable ligand, iminoglutaricsuccinic acid tetra sodium salt (IGS 4Na) was synthesised.

A mixture of 2.03 g (10 mmol) of ethyl β-aminoglutarate, 1.72g (10 mmol) of diethyl maleate and 0.4 ml of triethylamine is placed in a hermetically sealed round-bottomed flask at 32°C for 20 days. The reaction mixture (after 20 days) is extracted with 37 % hydrochloric acid solution (4 x 20 ml). The extract is basified with excess ammonia solution. The separated oil is extracted with chloroform (4 x 20 ml), which is then dried out magnesium sulphate (for 5 hours) and concentrated to give the IGS in its ester form. Product was characterised using spectroscopic techniques.

In an analogous way the ethyl groups of the ester were hydrolysed, yielding the sodium salt form of the ligand, according to the following reaction:

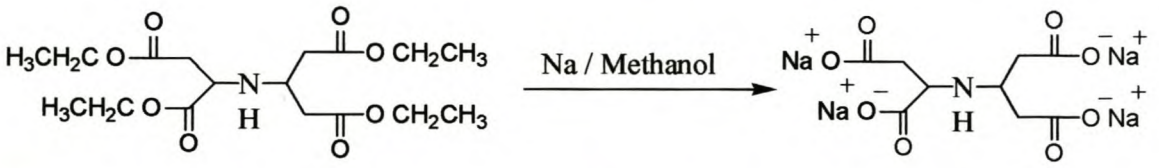


**Figure 3** Hydrolysis reaction of iminoglutaratesuccinate

## 2.3 Result and Discussion

### 2.3.1 Spectroscopic Characterisation of Ethyl β-Aminoglutarate (hydrochloride)

#### A Ethyl β-Aminoglutarate hydrochloride

As detailed in the experimental section, a recrystallised white crystal of ethyl β-aminoglutarate hydrochloride was recovered in a good yield of 13.5 g, 0.056mol, 70% (lit. 12 g, 0.05 mol, 62%); mp 84°C, (lit[1]. 82-84°C); $\delta_H$ (300 MHz, $CDCl_3$): 1.2 (t, 6H, $CH_3$), 3.0 (dd, 4H, $CH_2$-$CO_2C_2H_5$), 4.0 (m, 1H, $H_2N$-$CH$), 4.15 (q, 4H, $CO_2$-$CH_2$-$CH_3$), 8.6 (bs, 1H, NH); $\delta_C$ (75MHz, $CDCl_3$): 14 ($C_{1/1'}$), 36 ($C_{4,4'}$), 45 ($C_5$), 61 ($C_{2/2'}$), 171 ($C_{3/3'}$); MS: *m/z* 203 ($M^+$).

#### B Ethyl β-Aminoglutarate

According to the experimental section 2.2.1.1.1, a chloroform extract of the basified ethyl β-aminoglutarate hydrochloride, 11.5 g, 0.057 mol of ethyl β-aminoglutarate oil was recovered. $\delta_H$ (300 MHz, $CDCl_3$): 1.2 (t, 6H, $CH_3$), 1.65 (bs, 1H, NH), 2.4 (dd, 4H, $CH_2$-$CO_2C_2H_5$), 3.6 (m, 1H, NH-$CH$), 4.1 (q, 4H, $CO_2$-$CH_2$-$CH_3$); $\delta_C$ (75MHz, $CDCl_3$): 14 ($C_{1/1'}$), 42 ($C_{4/4'}$), 45 ($C_5$), 61 ($C_{2/2'}$), 172 ($C_{3/3'}$); IR (Neat): 3380 and 3308 (primary N-H stretch), 1731 (C=O stretch), 1151 (C-O stretch); MS: *m/z* 203 ($M^+$)

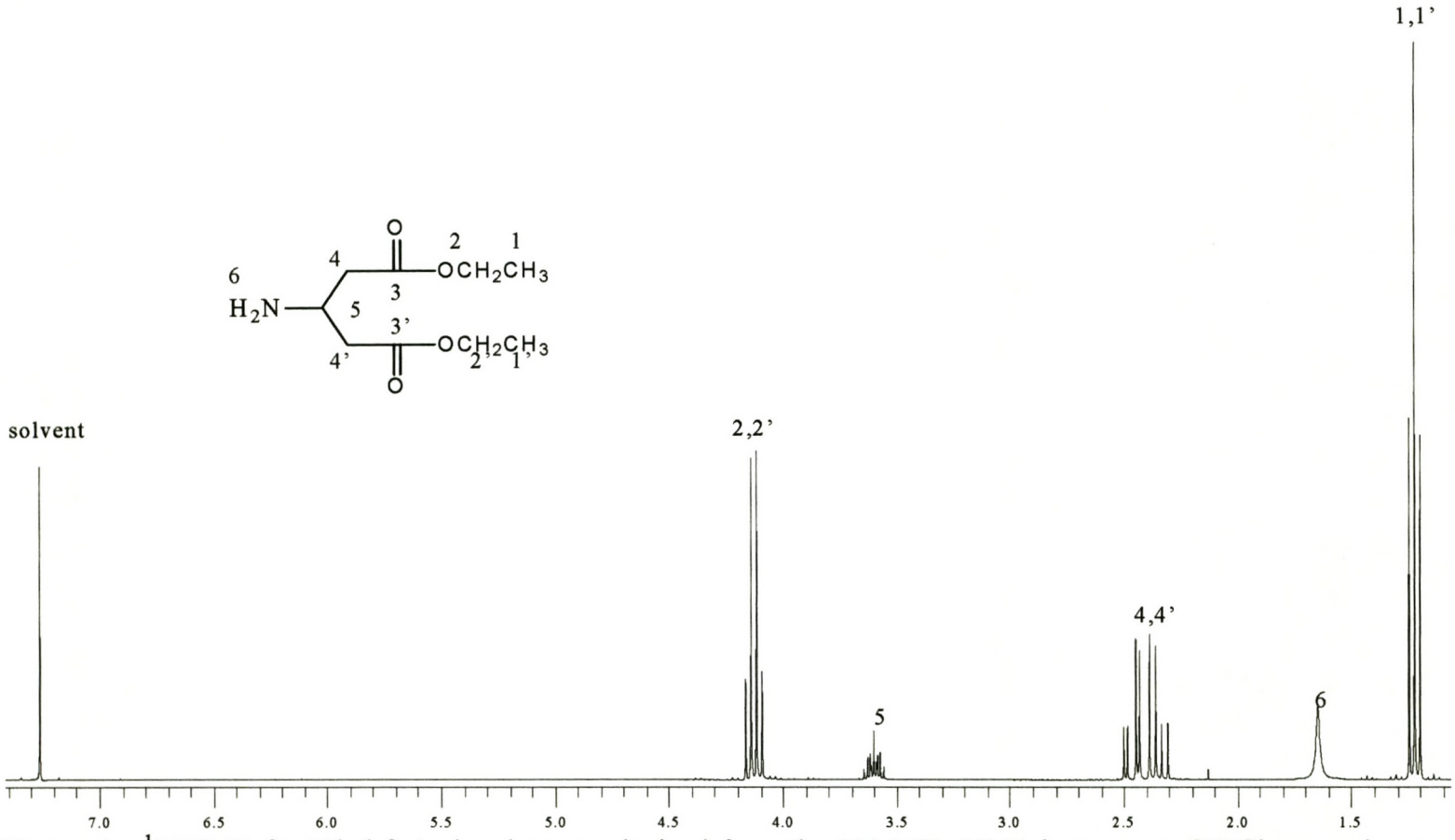


**Figure 4** $^{1}$H-NMR for Ethyl β-Aminoglutarate obtained from the 300 MHz NMR-instrument, $CH_3Cl$ as a solvent and TMS as internal reference

A comparison of the $^1$H-NMR spectra for the ethyl β-aminoglutarate hydrochloride (figure 27 refer to appendix) and ethyl β-aminoglutarate (figure 4), simply tells us to which atom the HCl is bonded (covalently). The major difference on both spectra is the position of the small broad peak due to the proton attached to the nitrogen. The peak is shifted far upfield from δ 8.6 ppm, in the case of β-aminoglutarate hydrochloride, to 2.4 ppm for the ethyl β-aminoglutarate. This clearly signifies that the N-atom was protonated by HCl.

The two dd signals at δ 2.3-2.5 and 2.8-3.15 in the proton spectra of the free and hydrochloride compounds respectively are due to the fact that the two protons in $C_{4/4'}$ are diastereoscopic, forming different dihedral angle with $H_5$. This results in the viccinal and geminal coupling , forming dd's for each $H_4$ proton and nine-line tt for $H_5$. (This explanation holds true in the case of IDG and IGS ligands both in their ester and tetra sodium salt forms).

### 2.3.2 Spectroscopic Characterization of Iminodiglutaric acid tetra sodium salt

According to the experimental section 2.2.2, iminodiglutarate was first synthesised, which upon hydrolysis gave the new potentially biodegradable ligand iminodiglutaric acid tetra sodium salt (IDG. 4Na).

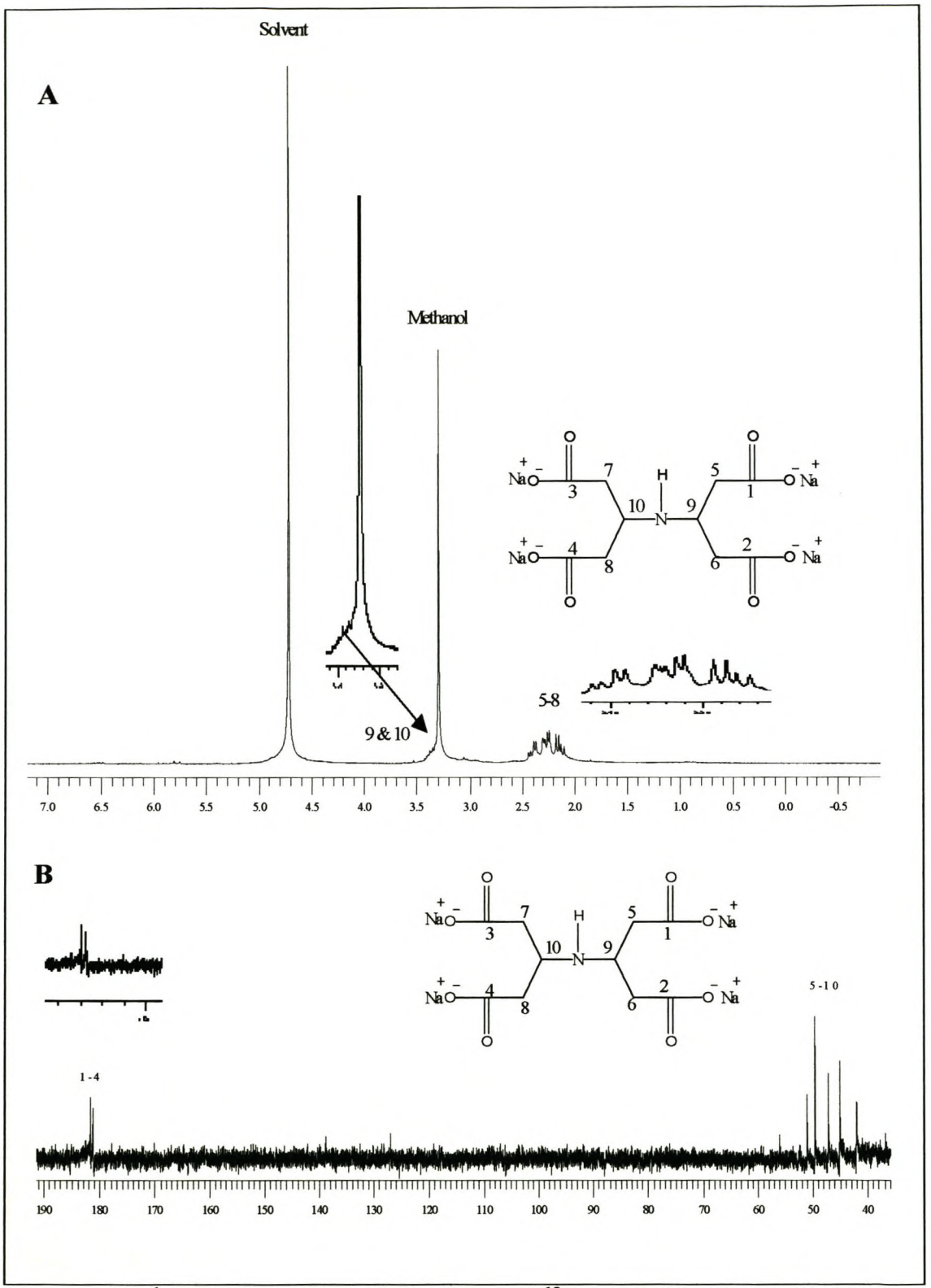


**Figure 5** (A) $^{1}$H-NMR spectrum of IDG 4Na; (B) $^{13}$C-NMR spectrum of IDG 4Na both obtained from the 300 MHz NMR-instrument, $D_2O$ as a solvent.

### (A) Tetraethyl Iminodiglutarate

The method reported by A.K. Saxena et al. (experimental section 2.2.2) yielded 7.5 g, 1.9 mmol (39.9%; lit[2] 38.6%). The spectra (Refer figure 29 in the appendix) obtained were almost identical with the ethyl β-aminoglutarate. This is due to the fact that iminodiglutarate is a perfectly symmetric compound with identical structure on both sides of an imaginary line of symmetry passing through the nitrogen atom. $\delta_H$ (300MHz, $CDCl_3$): 1.2 (t, 12H, $CH_3$), 1.9 (bs, 1H, NH), 2.4 (2 x dd, 8H, $CH_2$-$CO_2C_2H_5$), 3.6 (m, 2H, NH-*CH*), 4.1 (q, 8H, $CO_2$-$CH_2$-$CH_3$); $\delta_C$ (75MHz, $CDCl_3$): 15 ($C_1$), 42 ($C_4$), 46 ($C_5$), 61 ($C_2$), 173 ($C_3$).

### (B) Iminodiglutaric acid tetra sodium salt (IDG. 4Na)

Hydrolysis of iminodiglutarate (7 g, 18 mmol) gave 6.7 g (17.2 mmol) of iminodiglutaric acid tetrasodium salt (Figure 5). $\delta_H$ (300 MHz, $D_2O$): 2.1-2.45 (4 x dd, 8H, $CH_2$-$CO_2$), 3.2-3.5 (m, 2H, NH-*CH*-, $C_{9\ \&\ 10}$); $\delta_C$ (300MHz, $D_2O$): 42 - 52 ($C_{5\text{-}10}$ the tallest peak at δ 49.545 represents two overlapping peaks), 81 ($C_{1\text{-}4}$); IR (KBr plates): 3396 (O-H stretch H-bonded), 2956 ($sp^3$ C-H stretch), 1575 and 1405 (O=C—$O^-$ symmetric and asymmetric stretches)

The methanol peak, in the $^1$H-NMR spectrum, obscures the multiplet at δ 4.3ppm. The O-H hydrogen bonded broad peak was also manifested in the IR spectrum at 3396, which hides the N-H stretch in the IDG 4Na.

As it was expected, the key to identifying an ethyl ester, the quartet at 4.1 ppm and the associated triplet at 1.2 ppm in the $^1$H-NMR spectrum for iminodiglutarate vanished after the hydrolysis reaction in the $^1$H-NMR spectrum for iminodiglutaric acid tetra sodium salt which a clear indication for a complete hydrolysis reaction.

### 2.3.3 Spectroscopic Characterization of Iminodiglutaricsuccinic acid tetra sodium salt

As detailed in experimental section 2.2.3, iminoglutaricsuccinic acid tetra sodium salt was synthesised after hydrolysing iminoglutaratesuccinate. The spectroscopic results for both compounds follow:

#### (A) Tetraethyl Iminoglutaratesuccinate

1.5 g (4 mmol, 40%) of iminoglutaratesuccinate was obtained. For characterization $\delta_H$ (300 MHz, $CDCl_3$): 1.25 (2 x t, 12H, $CH_3$), 2.5 (dd, 6H, $CH_2$-$CO_2C_2H_5$), 3.4 ($q_n$, 1H, NH-*CH*), 3.7 (t, 1H, NH-*CH*-$CO_2C_2H_3$), 4.1 (3 x q, 8H, $CO_2$-$CH_2$-$CH_3$); $\delta_C$ (75 MHz, $CDCl_3$): 15 ($C_1$ 1 signal), 40 ($C_{4,7\ \&\ 11}$ 3 signal) 52 ($C_5$), 57 ($C_{10}$), 62 ($C_{2,9,13\ \&\ 14}$ 4 signal), 173 ($C_{3,8,12\ \&\ 15}$ 4 signal); MS: *m/z* 375 ($M^+$). (For the spectra, refer figure 30 in Appendix)

### (B) Iminoglutaricsuccinic acid tetra sodium salt (IGS.4Na)

Hydrolysis of tetraethyl iminoglutaratesuccinate (1.4 g, 3.7 mmol) gave 1.2 g (3.4 mmol) of iminoglutaricsuccinic acid tetra sodium salt. $\delta_H$ (300 MHz, $D_2O$): 2.0-2.5 (6 x dd, 6H, $CH_2$-$CO_2C_2H_5$), 3.2 ($q_n$, 1H, NH-*CH*-, $C_3$), 3.46 (t, 1H, NH-*CH*-, $C_7$); $\delta_C$ (75MHz, $D_2O$): 43 and 44 ($C_{2\ \&\ 5}$), 49.5 ($C_8$), 52.5 ($C_4$), 59.5 ($C_7$), 180-184 ($C_{1,\ 6,\ 9\ \&\ 10}$); IR (KBr plates): 3423 (O-H stretch H-bonded), 2957 ($sp^3$ C-H stretch), 1577 and 1404 (O=C—$O^-$ symmetric and asymmetric stretch).

The key peaks to identifying ethyl esters, the quartets at δ 4.1 ppm and the associated triplet at δ 1.25 ppm in the $^1$H-NMR spectrum for iminoglutaratesuccinate disappeared after the hydrolysis reaction in the $^1$H-NMR spectrum for iminoglutaricsuccinic acid tetra sodium salt. The absence of any peaks in these regions is a clear indication for the complete hydrolysis of the four ethyl groups in the four sites of the molecule. This means four Na metals substitute the four ethyl group.

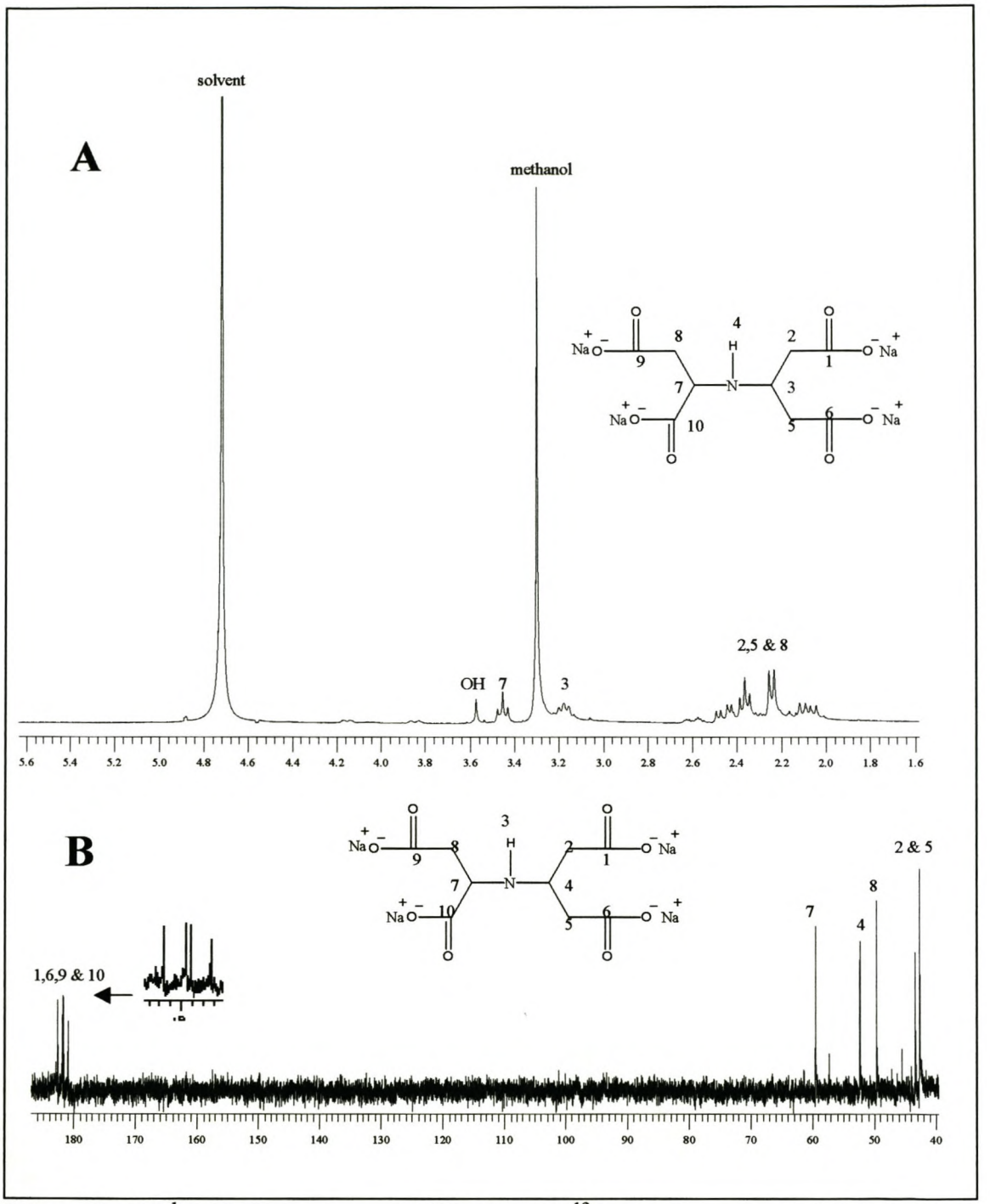


**Figure 6** (A) $^{1}$H-NMR spectrum of IGS 4Na; (B) $^{13}$C-NMR spectrum of IGS 4Na both obtained from the 300 MHz NMR-instrument, $D_2O$ as a solvent.

## References

1 W.A. Swarts, H. Feuer, *J. Am. Chem. Soc.*, 1955, **77**, 5427-8

2. A.K. Saxena, J. Rao, *Indian J. Chem.*, 1989, **28B**, 620-625

# Chapter Three

## Metal-Ligand Stability Constant Determination Using Cyclic Voltammetry

# 3 Metal-Ligand Stability Constant Determination Using Cyclic Voltammetry

## 3.1 General

Cyclic voltammetry (CV) has become a popular tool in the last fifteen years for studying electrochemical reactions.[1] It is perhaps the most versatile electrochemical technique for the study of electro-active species. Its versatility combined with the ease of measurement has resulted in extensive use of CV in the field of electrochemistry, inorganic chemistry, organic chemistry and biochemistry. The effectiveness of CV results from its capability for rapidly observing the redox behavior over a wide potential range.[2] It offers a rapid location of redox potentials of the electro-active species and an evaluation of the effect of media upon the process. Cyclic voltammetry curves have been ascribed for the characterization of complexes with low and large excess of ligands in pH dependent complex equilibria. Since multiple protonation and complex formation equilibria are involved during interactions of metals with ligands the employment of electrochemical techniques, such as CV, can be of great assistance in confirming the extent of the interaction between ligands and electroactive species (e.g. metal ions). Electrochemical techniques have found wide application in the characterization of complex ions in solution. Earlier treatment were limited by the assumptions that a reversible electrode reaction occure, i.e. a single complex in solution, and presence of a large excess ligand.[3, 4]

DeFord and Hume[5] extended the treatment to include step wise formation of complexes, and Schaap and McMasters [6] treated the case of mixed ligand complexes.

Organic chemists have applied the technique (CV) to the study of biosynthetic reaction pathways. An increasing number of inorganic chemists have been using cyclic voltammetry to evaluate the effect of ligands on the oxidation/reduction potential of the central metal ion in complexes and multinuclear clusters. [7] Killa has used CV to determine the stability constant of metal-complexes.[8]

## 3.2 Voltammetric Instrumentation

### 3.2.1 Electrochemical Cell of Cyclic Voltammetry

The cell is made up of three electrodes immersed in a solution containing an analyte and an excess of non-reactive electrolyte called a supporting electrolyte. (Figure 7) The physical design of the cell and the materials used in its construction must be chosen with both the nature of the sample and experimental objectives in mind.

The three electrodes are:

- Working electrode ( Microelectrode)
- Reference electrode
- Counter (Auxiliary) electrode

### 3.2.1.1 Working Electrode (Microelectrode)

The working electrode (macro and micro) in an electrochemical arrangement is the electrode at which the analyte is reduced or oxidized. In other words it is an electrode at which the reaction of interest takes place.

In the early 1970s a number of research groups exploited the advantages of microelectrodes, which are normally defined as devices with characteristic dimensions smaller than about 20 μm, over conventional electrodes.[9] The microelectrode employed in voltammetry takes a variety of shapes and forms. Often, they are small flat disc of a conductor that are press-fitted into a rod of an inert material, such as Teflon, that has a wire contact imbedded in it.[10] The conductor could be of different materials (e.g. platinum, gold or glassy carbon).

Advantages of microelectrodes over the conventional electrode are:

- Very low current can be measured with relative ease,
- Capacitative charging currents, the limiting factor in all transient electrochemical techniques, are reduced to insignificant proportions, [9]
- The rate of mass transport to and from the electrodes increase as the electrode size decreases [9,11]

As a consequence of reduced capacitative charging current and increased mass transport rate, microelectrodes exhibit excellent signal-to-noise ratio (S/N) characteristics.

Finally the small size of microelectrodes is an obvious feature, which allows further reduction of the necessary sample volume. They are easily implemented and involve relatively low costs.

The potential range that can be used with these electrodes depends not only on the electrode material but also on the composition of the solution in which it is immersed. Generally, oxidation of water develops positive potential limitations and negative limits arise from the reduction of water. Oxidation of water gives molecular oxygen and reduction of water gives hydrogen. But, due to the high overvoltage of hydrogen on mercury, Mercury electrode can tolerate relatively large negative potentials.[10]

Mercury electrodes have been employed in voltammetry for several more reasons:

- It has a relatively large negative potential range
- A fresh metallic surface is readily formed by simply producing a new drop
- Many metals are reversibly reduced to amalgams at the surface of mercury electrode, which simplifies the chemistry

This includes: Mercury film electrode (MFE), Hanging mercury drop electrode (HMDE), dropping mercury electrode (DME), streaming mercury electrode (SME), and static mercury drop electrode (SMDE). The simplest of these is MFE formed by electron deposition of the metal on to a disc electrode. MFE was employed in this study.

#### 3.2.1.2 Reference Electrode

The potential of this electrode remains constant through-out the experiment. This electrode is insensitive to the composition of the solution under study. Ag/AgCl, and saturated calomel (SCE) are favourite candidates of reference electrode. The former was employed in this study.

### 3.2.1.3 Counter (Auxiliary) Electrode

This electrode is coupled to the working electrode but plays no part in determining the magnitude of the potential being measured. This electrode, usually platinum wire or a pool of mercury, serves to conduct electricity from the source through the solution to the working electrode.[10] Platinum wire was employed in this work.

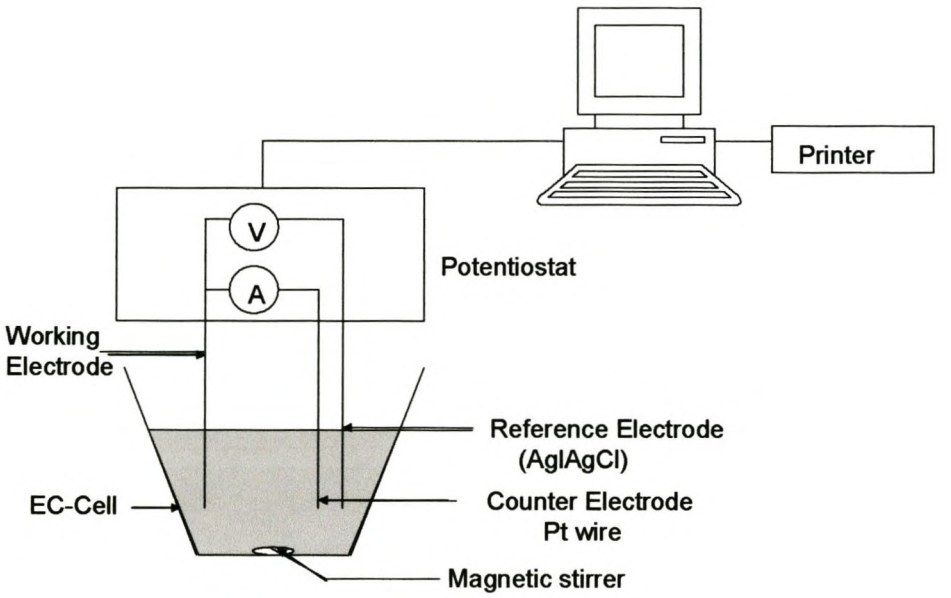


**Figure 7** A simplified diagram for voltammetic experiments

## 3.3 Fundamentals of Cyclic Voltammetry

CV consists of cycling the potential of the working electrode, which is immersed in unstirred solution, and measuring the resulting current. The potential of this working electrode is controlled versus the reference electrode, saturated calomel electrode (SCE) or the silver/silver chloride (Ag/AgCl) electrode. The controlling potential which is applied across these two electrodes can be considered an excitation signal. The excitation signal for CV is a linear potential scan with a triangular wave form [2] as shown in figure 8. The voltage applied to the working electrode is scanned nearly from the initial value, *initial E*, to a predetermined limit, *high E*, (known as the switching potential) where the direction of the scan is reversed. The operator can stop the scan or let it scan between the *high E* and some other pre-selected value, *low E*. [12]

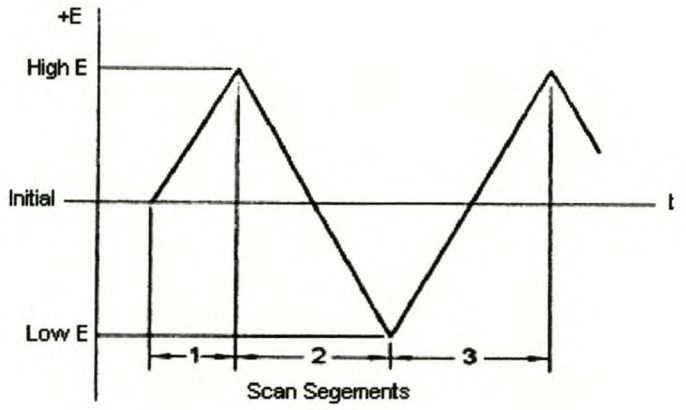


**Figure 8** Typical excitation signal for cyclic voltammetry- triangular potential waveform

Hence in this technique, the potential of the stationary working electrode in a quiescent solution is scanned linearly using a triangular potential waveform, and the current resulting from the applied potential measured. [13, 14] The resulting plot of current versus potential is termed a cyclic voltammogram (figure 9). The current-potential curve is the electrochemical equivalent of a spectrum obtained in spectrophotometry.[2, 12]

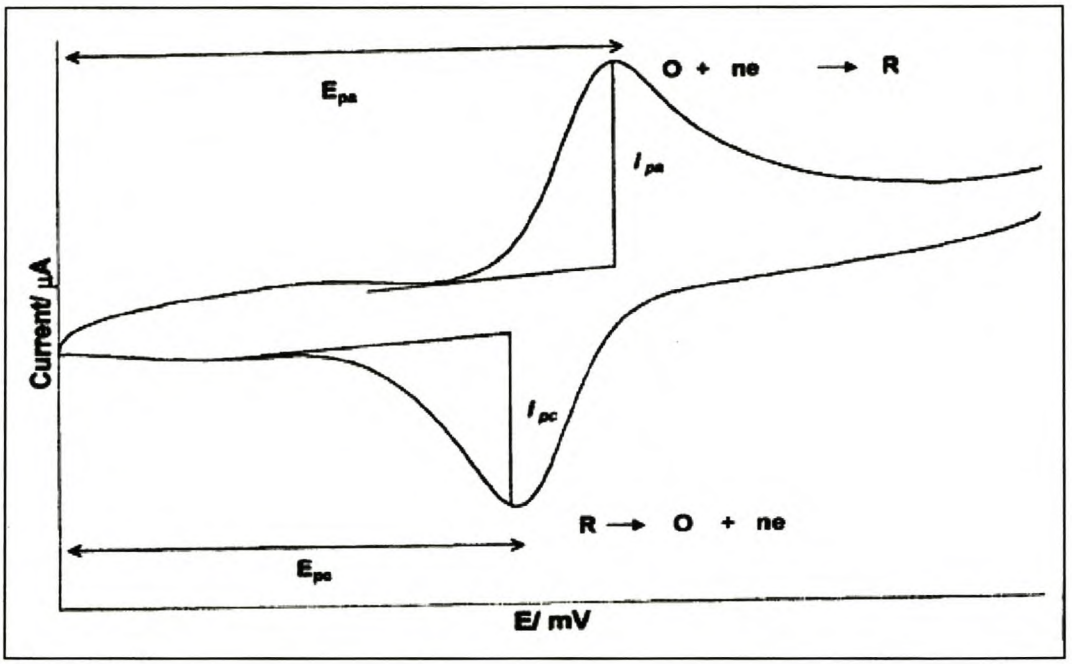


**Figure 9** Typical Cyclic Voltammogram

The information that could be obtained from cyclic voltammogram are:

- anodic ($i_{pa}$), and cathodic ($i_{pc}$) peak currents, which is directly proportional to the concentration of the analyte (although the presence of the background charging current in CV limits its usefulness for qualitative analysis), and
- anodic ($E_{pa}$) and cathodic ($E_{pc}$) peak potentials, which appear at the characteristic

positions of the particular analytes in the matrix.

One method for measuring $i_p$ involves extrapolation of a baseline current as shown in the figure. The establishment of a correct baseline is essential for the accurate measurement of peak currents which is not always easy, particularly for more complicated systems.[2]

Depending on the speed of the electron exchange of the redox species, the voltammetric process could be reversible, quasi-reversible or irreversible.

By reversible, electrochemists mean that the reaction is fast enough to maintain the concentrations of the oxidized and reduced forms in equilibrium with each other at the electrode surface. [15]The proper equilibrium ratio at a given potential is determined by the Nernst Equation:

$$E = E^{o} - RT/nF \ \ln([R]/[O])_{x=0} \qquad \textbf{3.1}$$

Where, O and R are the oxidized and the reduced forms of the species respectively.

The formal reduction potential, $E^{o}$, for a reversible couple, is given by:

$$E^{o} = (E_{pa} - E_{pc})/ 2 \qquad \textbf{3.2}$$

The number of the electrons transferred in the electrode reaction (n) for a reversible couple can be determined from separation between the peak potentials:

$$\Delta E_p = E_{pa} - E_{pc} \approx 0.059/n \qquad \textbf{3.3}$$

According to Randles-Sevcik equation,

$$i_p = (2.69 \times 10^5) n^{3/2} A D^{1/2} C \upsilon^{1/2} \qquad \textbf{3.4}$$

Where $i_p$ is peak current (A), n is electron stoichiometry, A is electrode area ($cm^2$), D is diffusion coefficient ($cm^2/s$), C is concentration ($mol/cm^3$), and $\upsilon$ is scan rate (V/s). Accordingly, $i_p$ increases with $\upsilon^{1/2}$ and is directly proportional to concentration. For a simple reversible couple, the magnitude of $i_{pa}$ is equal to $i_{pc}$.

In case of the irreversible cyclic voltammogram a single oxidation or reduction peak with no reverse wave is observed. Electrochemical irreversibility is caused by slow electron exchange of the redox species with the working electrode. Hence, the above equations (3.1-3.4) are not applicable in case of irreversible electrochemical processes. Electrochemical irreversibility is characterized by a separation of peak potentials greater than indicated by Eq. 3.3. Redox couple whose peaks shift farther apart with increasing scan rate are categorized as quasi-reversible (some authors merely say irreversible).

## 3.4 Voltammetric Study of Selected Heavy Metals ( $Cu^{2+}$, $Zn^{2+}$ and $Cd^{2+}$) with the Ligands-IDG and IGS

### 3.4.1 Experimental Section

#### 3.4.1.1 Instrumentation

All the experiments were performed with the BAS C2 and C3 cell stand attached to a BAS100B system potentiostat (electrochemical analyser). The three electrode electrochemical cell system comprises: a mercury thin film coated carbon microelectrode as working electrode, a platinum wire as counter electrode and a Ag/AgCl as auxiliary or reference electrode. The pH measurements were conducted using the JENWAY model 4330 pH / conductivity meter. High purity nitrogen was used for deaeration of the sample solution.

General parameters used throughout the study are given below (T=25°C)

| | |
|---|---|
| Initial potential (mV) | -200 |
| High potential (mV) | -200 |
| Low potential (mV) | -2000 |
| Scan rate (mV/s) | 100 |
| Initial Direction | Negative |
| Number of Segments | 2 |
| Sensitivity (nA/V) | 100 |

### 3.4.1.2 Materials

Chemicals and electrolyte used were of the analytical or highest commercially available grade. The water used for preparing the solutions was first distilled and then ultra purified using the Milli-Q purification system.

| CHEMICALS | COMPANY and GRADE |
|---|---|
| Copper solution (1000 ppm) (in nitric acid) | Fluka (Atomic spectroscopy standard solution) |
| Zinc solution (1000 ppm) (in nitric acid) | Fluka (Atomic spectroscopy standard solution) |
| Cadmium solution (1000 ppm) (in nitric acid) | Fluka (Atomic spectroscopy standard solution) |
| Lead solution (1000 ppm) | Fluka (Atomic spectroscopy standard solution) |
| Iminodiglutaricacid tetrasodium salt (IDG-4Na) | Synthesised in our laboratory |
| Iminoglutaricsuccinic-tetra sodium salt (IGS-4Na) | Synthesised in our laboratory |
| Ammonia solution ($NH_3$) | Merck (33%) |
| Hydrochloric acid solution (HCl) | SAAR Chem (32%) |
| Nitric Acid ($HNO_3$) | Merck (65%) Suprapure |
| Mercury metal triple-distilled | SAAR Chem (univar) |

**Table 2.** Chemicals used and grades

### 3.4.1.3 Preparation of solutions

#### (A) Standard preparations

**Copper**, 3.45 x $10^{-4}$ M. A volume of 1.0 ml of a 1000 ppm copper stock solution was diluted to the mark with 0.1 M $NH_3$ solution in a 100 ml volumetric flask.

**Cadmium**, 2.08 x $10^{-4}$ M. A volume of 1.0ml of a 1000 ppm cadmium stock solution was diluted to the mark with 0.1 M $NH_3$ solution in a 100 ml volumetric flask.

**Zinc**, 3.33 x $10^{-4}$ M. A volume of 1.0 ml of a 1000 ppm lead stock solution was diluted to the mark with 0.1 M $NH_3$ solution in a 100 ml volumetric flask.

#### (B) Other solutions

**$NH_3$ solution**, 0.1 M. A volume of 2.90 ml of ammonia solution was diluted to the mark with ultra pure water in a 500 ml volumetric flask.

**HCl solution**, 0.1 M. A volume of 0.83 ml of hydrochloric acid solution was diluted to the mark with ultra pure water in a 100 ml volumetric flask.

**Mercury solution**, 0.015 M $Hg^{2+}$ 0.3 g of triple distilled mercury was dissolved with few drops of concentrated nitric acid solution and was diluted to the mark with ultra pure water in 100 ml volumetric flask.

**IDG-4Na solution**, 0.01 M. 0.09125 g of the ligand was weighed into a 25 ml volumetric flask and made up to the mark with 0.1 M $NH_3$ solution.

**IGS-4Na solution**, 0.01 M. 0.0176 g of the ligand was weighed in to a 25 ml volumetric flask and made up to the mark with 0.1 M $NH_3$ solution

### 3.4.1.4 General Procedure

10 ml of 0.015 M mercury solution was placed in an electrochemical cell. A thin mercury film was coated on the carbon microelectrode (11 Mm) using DPSV stripping technique at -200 mV initial and -2000 mV final potentials and 400 rpm for 10 minutes. A background voltammogram was first recorded for the 0.1 M $NH_3$ buffer solution. Before each metal-ligand complexation study, a voltammogram for each metal ion was obtained. Metal-ligand complexation was then examined as follows: 10 ml of $Cu^{2+}$, $Cd^{2+}$ and $Zn^{2+}$ stock solutions each were used, to which were added aliquots of appropriate ligand standard solution to ensure a 1:1 ratio of metal:ligand. Thereafter, aliquots of 0.1 M HCl were added to study the species formed at different pH. Before each experimental run, the solution in the electrochemical cell was deaerated with pure nitrogen gas for at least 10 minutes.

### 3.4.1.5 Treatment of Voltammetric data

Metal complexation was investigated for the pentadentate polyaminocarboxylate agent

$H_4IDG$ and $H_4IGS$ with $Cu^{2+}$, $Cd^{2+}$ and $Zn^{2+}$, according to the experimental procedure mentioned in the preceding section.

For calculating the metal ligand formation constant, information, regarding the change in the reduction potential ($\Delta E$) with the change in the pH of the solution in the electrochemical cell, can be obtained from the voltammograms run during the complexation study. Change of the reduction potential ($\Delta E$) represents a shift in a peak potential observed from CV experiment at each pH value to which the metal ligand system is adjusted in the electrochemical cell. The complex stability (formation) constant can be determined by plotting the change in the reduction potential ($\Delta E$) against solution pH, which follows directly from the modification of the Lingane equation: [16]

$$\Delta E = -RT/nF \ln [ML]/[M][LH_x] + 2.303x/n \ pH \qquad \textbf{3.5}$$

The above equation is derived from the following Nernst Equation

$$E = E^{o} - RT/nF \ln K \qquad (a)$$

For reactions like:

$$M^{+} + LH_X \longrightarrow ML + xH^{+}$$

the equilibrium constant K is used to describe the stability of such a metal-ligand complex, It is defined as:

$$K = [ML][H^+]^x/[M][LH_x] \qquad (b)$$

Substituting Eqn (b) in Eqn (a) we get:

$$E = E^o - RT/nF \ln[ML][H^+]^x / [M][LH_x]$$

Or

$$\Delta E = - RT/nF \ln[ML] / [M][LH_x] - RT/nF \ln[H^+]^x \qquad (c)$$

But we know that $\ln x = \log_e x$

$$\Delta E = - RT/nF \ln[ML] / [M][LH_x] - 2.303.x/n \log[H^+] \qquad (d)$$

But $\log[H^+] = pH$, hence

$$\Delta E = - RT/nF \ln[ML] / [M][LH_x] - 2.303.x/n \ pH \qquad (f)$$

Or it can be rearranged to:

$$\ln K = nF/RT [2.303/n \ pH - \Delta E ] \qquad \textbf{3.6}$$

This modified Lingane's equation was used to determine the stability constant. Slop changes in the curve of the ΔE vs pH plot, due to the formation of different equilibria at different pHs, corresponds to the logK value for the complex and can be read directly off the graph. A similar approach relating to the modified Lingane equation has been

followed by Cukrowski et al. in their polarographic study of formation curve for complexes at a fixed ligand:metal ratio and varied pH [17, 18] and by Crouch et al. using cyclic voltammetry. [16]

### 3.4.2 Voltammetric Study of Selected Heavy Metals ($Cu^{2+}$, $Zn^{2+}$ and $Cd^{2+}$) with Iminodiglutaric Acid (IDG)

All the experiments were performed according to the procedure detailed in section 3.4.1.4.

#### 3.4.2.1 Result and Discussion

The metal complexation was investigated for the tetra sodium salt form of pentadentate new polyaminocarboxylate agent, IDG, and $Cu^{2+}$, $Cd^{2+}$ and $Zn^{2+}$.

The following complex is formed when IDG is reacted with any of these metals

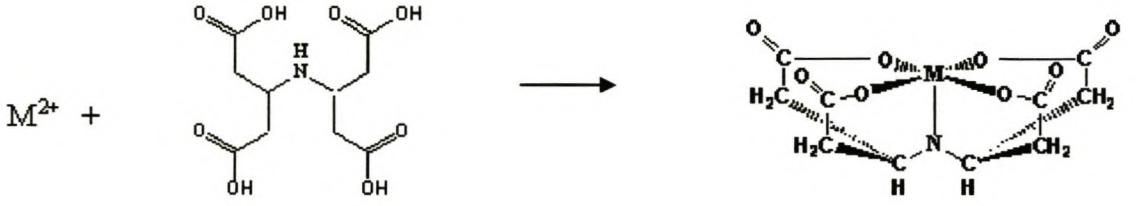


**Figure 10** Metal-IDG complexation reaction

The complex stability (formation) constants of $H_4IDG$ with $Cu^{2+}$, $Cd^{2+}$ and $Zn^{2+}$ were determined at the surface of a thin mercury film coated glassy carbon microelectrode (11

μm). Ag/AgCl and Pt wire were used as reference and auxiliary electrodes respectively.

### 3.4.2.1.1 Study of Zinc (II) and its IDG complex

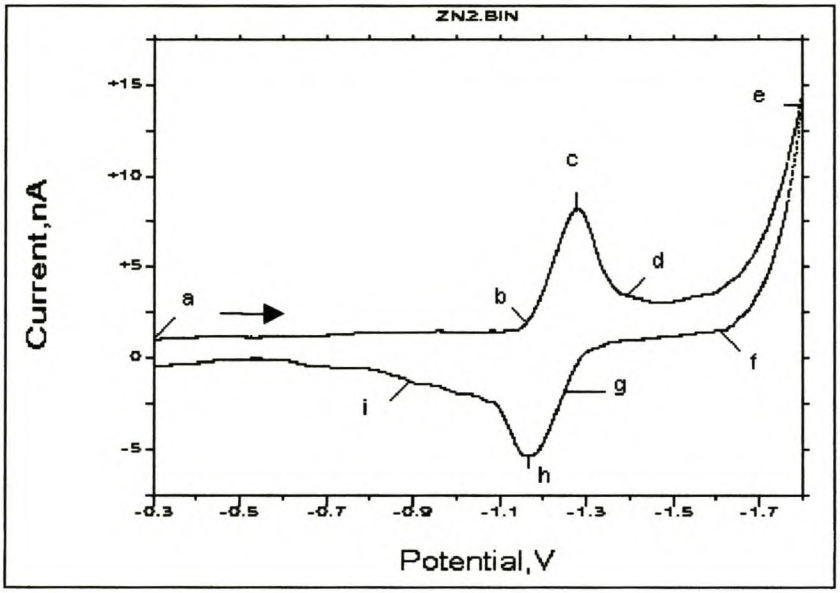


**Figure 11** cyclic voltammogram of Zinc at pH 10.3, in 0.1 M ammonia buffer, T = 25°C, thin film mercury coated carbon microelectrode; scan rate = 100 mV/s

Shown in figure 11 is a quasi-reversible cyclic voltammogram of the $Zn^{2+}$ion solution. The CV run imposes a linear sweep in a negative direction, which is called a cathodic or reductive sweep, followed by a reverse sweep in the opposite (positive) direction which is called the anodic or the oxidative sweep.

The potential is scanned, as indicated by an arrow, negatively, forward scan, from the initial potential –0.20 V (a) When the potential is sufficiently negative to the $Zn^{2+}$

cathodic current is indicated at (b) due to the electrode process

$$Zn^{2+} + 2e^- \longrightarrow Zn$$

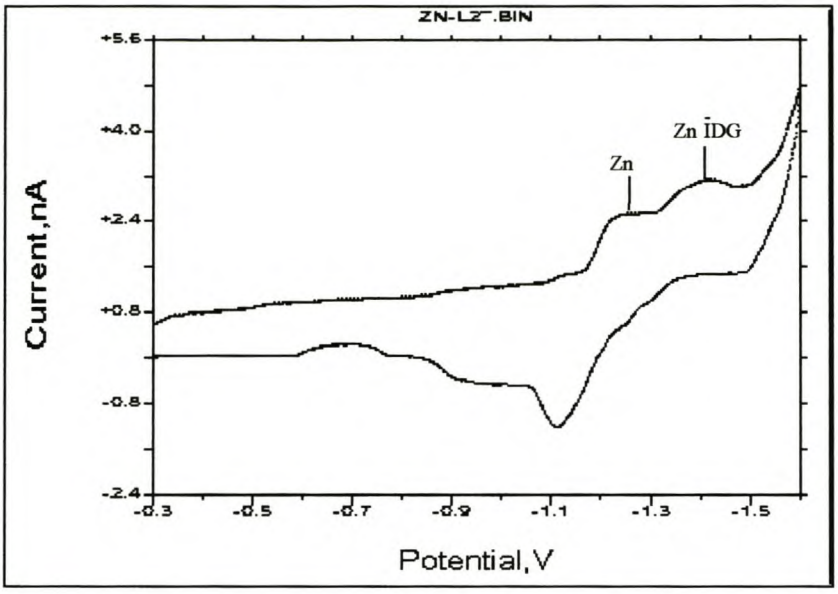


**Figure 12** Cyclic voltammogram of $Zn^{2+}$-IDG at pH 9 in 0.1M ammonia buffer, T= 25oC,thin film mercury coated carbon electrode scan rate = 100mV/s

The electrode is now a sufficiently strong reductant to reduce $Zn^{2+}$. Figure 11 shows the quasi-reversible behaviour for the $Zn^{2+}$/Zn redox couple. During the cathodic sweep, a defined peak is observed at a potential of -1.28V. Hence this potential is the reduction potential for $Zn^{2+}$. The cathodic current increases rapidly (b→c) until the concentration of $Zn^{2+}$ at the electrode surface substantially diminish, causing the current to peak (c). The current then decays (c→f) as the solution surrounding the electrode is depleted of $Zn^{2+}$ due to its electrolytic conversion to Zn. The scan direction is switched to positive (oxidative) sweep at –0.20 V (e) for the reverse scan.

During the reverse scan when the electrode becomes a sufficiently strong oxidant, the

electrode process (shown below) can now oxidize Zn, which has been accumulated adjacent to the electrode

$$Zn \longrightarrow Zn^{2+} + 2e$$

This electrode process causes anodic current (g→I). The cathodic peak rapidly increases until the surface concentration of the Zn is diminished, causing the current to peak (h). The current then decays (h→i) as the solution surrounding the electrode is depleted of Zn. Cycle is completed when it reaches +0.20 V. This potential was chosen as an initial potential to avoid any electrolysis of $Zn^{2+}$ when the electrode is switched on.

The peak at the potential of -1.41V, in Figure 12 cyclic voltammogram, is obtained after adding aliquots of the appropriate ligand standard solution (0.01 M IDG) to the electrochemical cell containing the metal ion solution. This potential corresponds to the reduction potential of the [Zn-$IDG^{2-}$] complex. This voltammogram shows an irreversible behaviour for the complex. After the addition of aliquots of ligand, a decrease in the metal peak was observed and the metal-ligand peak appeared on the more negative potential at the pH of 9. This is because complexes, due to the shielding effect of the overall negative electron charge of the complex, have greater resistance to reduction. Thereafter, aliquots of 0.1 M HCl were added to decrease the pH of the solution. As the pH decreases further, there would be a strong competition of the proton ions in the electrochemical cell solution with the metal for the active sites of the ligand. Hence there is simultaneous "step-wise" removal of the metal, and protonation of the ligand. This "step wise" decomplexation is manifested on the gradient changes in the graph of change in potential (ΔE) against pH. (Figure 13)

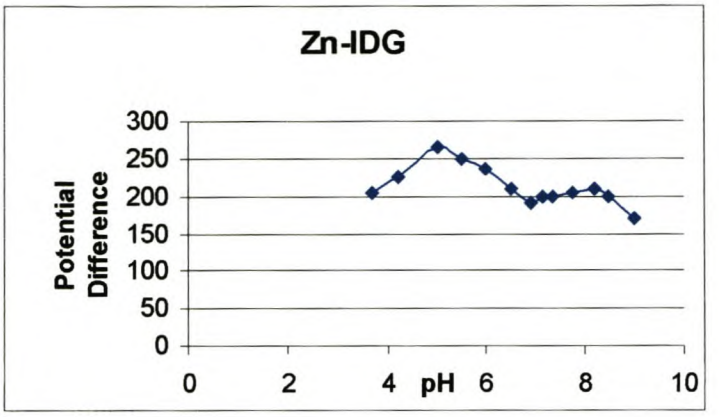


**Figure 13** Plot of ΔE vs. pH for determination of stability constants, in pH 10.3 ammonia buffer (I=0.1 M, T = 25°C)

The modified Lingane equation (Eq.3.5) was used to calculate the value of the stability constant for the Zn-$IDG^{2-}$ complex. In this case, the stability constant was determined from figure 13. The changes in the gradient of such plots correspond to the logK values for the complex and can be read directly off the graph. From the graph three changes in gradients can be read at pH 5, 6.9, and 8.23, which correspond to the step-wise formation constants, $\log K_1$, $\log K_2$ and $\log K_3$ respectively. The logarithm of the overall formation constant ($\log K_f$) is the summation of these values, ($\log K_f = \log K_1 + \log K_2 + \log K_3 = 20.13$). A similar approach and cyclic voltammogram explanations holds true for the other metal ions and their metal ligand complexes. Table 4 summarizes the step wise and overall formation constants for complexes of IDG with the selected metal ions investigated.

### 3.4.2.1.2 Study of Cadmium(II) and its IDG complex.

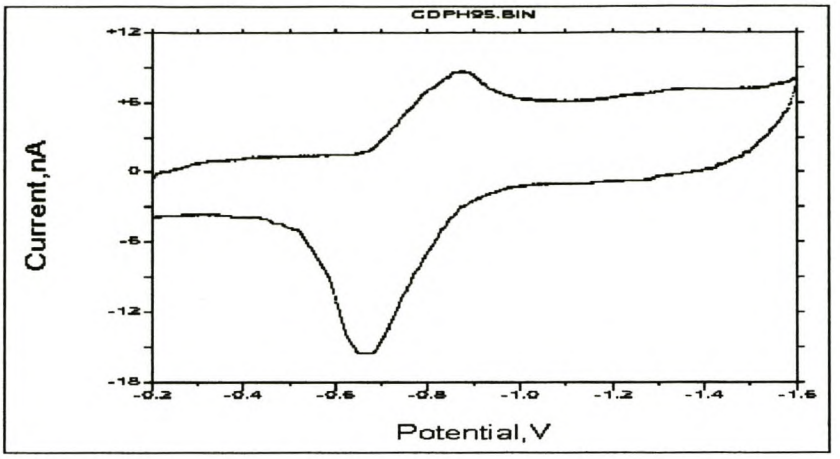


**Figure.14** Cyclic Voltammogram of Cd at pH 10.3 in 0.1 M ammonia buffer, T = 25°C, thin film mercury coated carbon microelectrode, scan rate = 100 mV/s

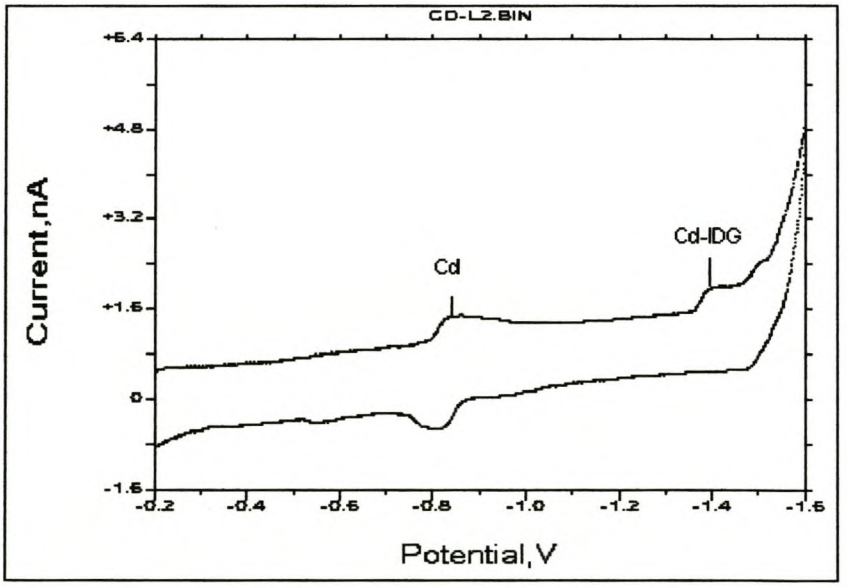


**Figure 15** Cyclic Voltammogram of Cd-IDG at pH 10.3 in 0.1 M ammonia buffer, T = 25°C, thin film mercury coated carbon microelectrode, scan rate = 100 mV/s

Shown in figure 14 and 15 are the cyclic voltammograms of the $Cd^{2+}$/Cd redox couple

and the $Cd^{2+}$-$H_4IDG$ complex at pH 10 and 10.37 respectively. The reduction peak for the cadmium ion at Cd (Hg) is at the potential of –8.75 V. In figure 15 a cyclic voltammogram for $Cd^{2+}$-$H_4IDG$ obtained after the addition of aliquots of 0.01 M IDG, shows a peak at the potential –1.40 V due to the stable complexation between the metal ion and the ligand. By decreasing the pH of the solution from 10.37 far down to 1.3, the simultaneous stepwise de-complexation and protonation of the ligand was studied carefully on addition of appropriate amounts of 0.1 M HCl. From the plot of the difference in potential of the metal-ligand peak and the metal peak (ΔE) against the pH of the solution (Figure 16), the major changes on the gradient can be identified at 5.7, 7, and 9 which correspond to the step wise formation constants of the different species.

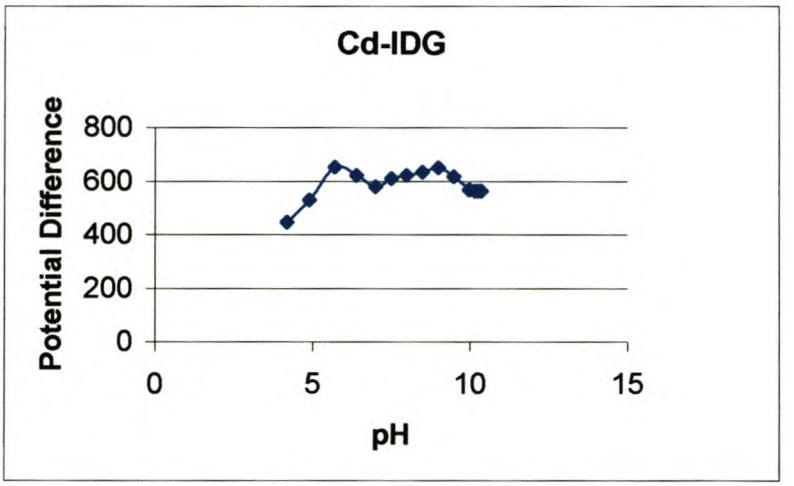


**Figure 16** Plot of ΔE vs. pH for determination of stability constants for Cd-IDG, in pH 10.3 ammonia buffer (I=0.1 M, T = 25°C)

### 3.4.2.1.3 Study of Copper (II) and its IDG complex

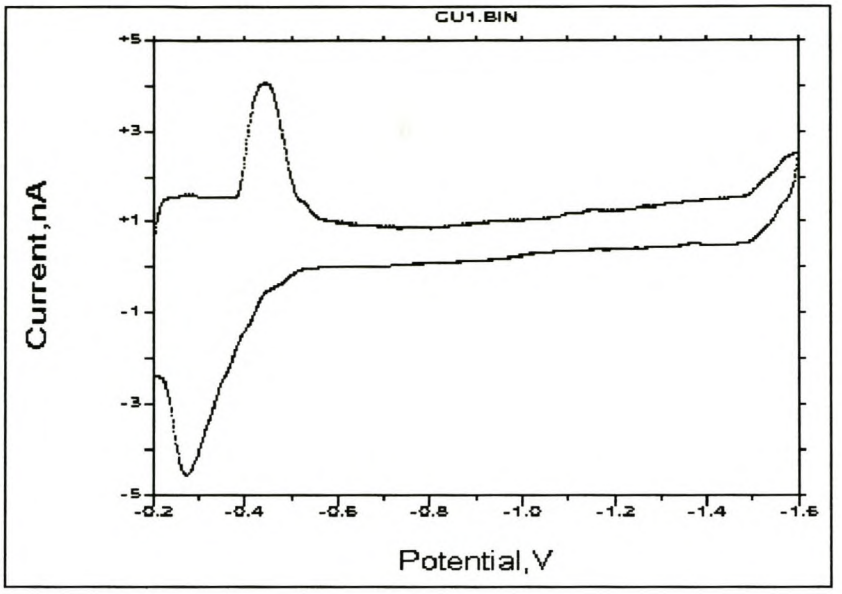


**Figure 17** Cyclic Voltammogram of Cu at pH 10.3 in 0.1 M ammonia buffer, T = 25°C, thin film mercury coated carbon microelectrode, scan rate = 100 mV/s

A quasi-reversible cyclic voltammogram for $Cu^{2+}$/Cu redox couple is shown in Figure 17. At a potential around -400 mV, the electrode becomes sufficiently strong enough to reduce $Cu^{2+}$ to $Cu^{o}$. When the electrode is sufficiently negative to the $Cu^{2+}$ cathodic current a peak emerged due to the following electrode process

$$Cu^{2+} + 2e^{-} \longrightarrow Cu$$

The reduction potential for the free metal ion is –447 mV. at pH of 10.3. The peak at the

potential of –1.43 V in figure 18 is due to the complexation of copper with the ligand and hence it belongs to the metal ligand ($Cu\text{-}IDG^{2-}$) peak. It was obtained after the addition of aliquots of 0.01 M IDG to ensure a 1:1 ratio, at the pH of 10.3. With the formation of the complex, the peak height for the metal ion was observed to decrease.

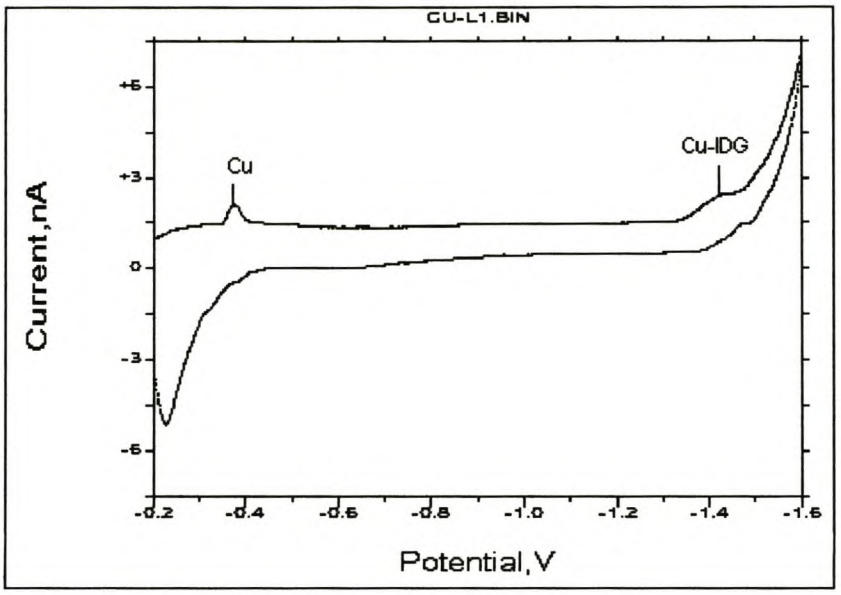


**Figure 18** Cyclic Voltammogram of Cu-IDG at pH 10.3 in 0.1 M ammonia buffer, T = 25°C, thin film mercury coated carbon microelectrode, scan rate = 100 mV/s

From Figure 19, the major changes are at pHs 5.31, 8.4 and 9.5. The large change in the graph signifies the different species of Cu with the complex. Each of this pH values correspond to the step-wise logK values of the complexation processes of the $Cu\text{-}IDG^{2-}$ complex.

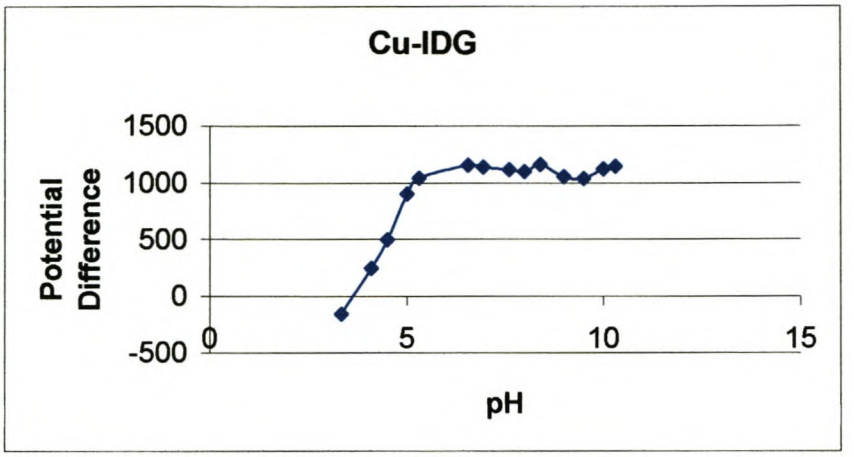


**Figure19** Plot of ΔE vs. pH for determination of stability constants, in pH 10.3 ammonia buffer (I=0.1 M, T = 25°C)

| Metal Ion | Peak Potential (mV) | |
|---|---|---|
| | Metal Ion | Metal Ligand* Complex |
| Copper(II) | -447 | -1428 |
| Cadmium(II) | -875 | -1402 |
| Zinc(II) | -1276 | -1412 |

* The ligand = IDG

**Table 3** Peak potentials for free metal ions and metal-IDG complexes

| Metal | Logarithm of the Stability Constants | | | |
|---|---|---|---|---|
| | $\log K_1$ | $\log K_2$ | $\log K_3$ | $\Sigma \log K_f$ |
| $Zn^{2+}$ | 5.00 | 6.90 | 8.20 | 20.10 |
| $Cd^{2+}$ | 5.70 | 7.00 | 9.00 | 21.70 |
| $Cu^{2+}$ | 5.31 | 8.40 | 9.50 | 23.21 |

**Table 4** The complex stability constants of $Zn^{2+}$, $Cd^{2+}$ and $Cu^{2+}$ with $H_4IDG$

| Ligands | Metals | | |
|---|---|---|---|
| | Zn $LogK_f$ | Cd $LogK_f$ | Cu $LogK_f$ |
| **EDTA** | 18.26 | 18.26 | 20.54 |
| **EDDS** | 15.25 | 12.56 | 20.12 |
| **DTPA** | 20.49 | 21.2 | 23.58 |
| **NTA** | 11.98 | 11.10 | 14.42 |

**Table 5** Literature values for complex stability constants of $Zn^{2+}$, $Cd^{2+}$ and $Cu^{2+}$ with different APCA ligands [19]

The relative stability of the 1:1 metal complexes were found to increase in the order of ZnIDG < CdIDG < CuIDG, which is, roughly, in agreement with the Irving-Williams* order of stability for complexation between transition metal ions and chelating agents. The values of these stability constants reflect the strength of complexation: the higher the stability constant, the more favourable the formation of the complex is, or the stronger the complex is.

* For first row divalent metal ions $Ba^{2+} < Sr^{2+} < Ca^{2+} < Mg^{2+} < Mn^{2+} < Fe^{2+} < Co^{2+} < Ni^{2+} < Cu^{2+} > Zn^{2+}$

### 3.4.3 Voltammetric Study of Selected Heavy Metals ($Cu2^{+}$, $Zn^{2+}$ and $Cd^{2+}$) with Iminoglutaricsuccinic Acid (IGS)

Experimental procedure detailed in section 3.4.1.4 was strictly followed for the metal-IGS complexation study.

#### 3.4.3.1 Result and Discussion

The metal:ligand complexation was investigated for the tetra sodium salt form of pentadentate new polyaminocarboxylate agent, IGS, and $Cu^{2+}$, $Cd^{2+}$ and $Zn^{2+}$.

Example of the complexation reaction - metal:IGS - is demonstrated in figure 20.

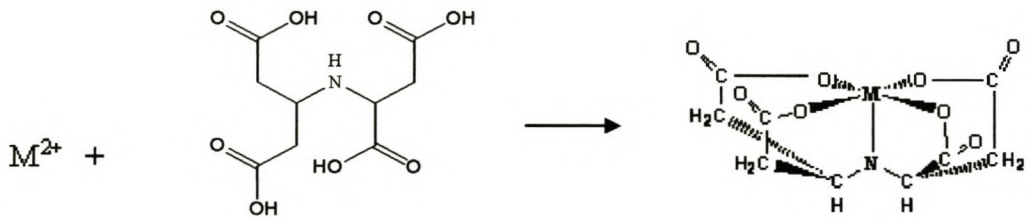


**Figure.20** Metal-IGS complexation reaction

The complex stability (formation) constants of $H_4IGS$ with $Cu^{2+}$, $Cd^{2+}$ and $Zn^{2}$ were determined at the surface of a thin mercury film coated glassy carbon microelectrode (11

μm). Ag/AgCl and Pt wire were used as reference and auxiliary electrodes respectively.

### 3.4.3.1.1 Study of Zinc(II) and its IGS complex

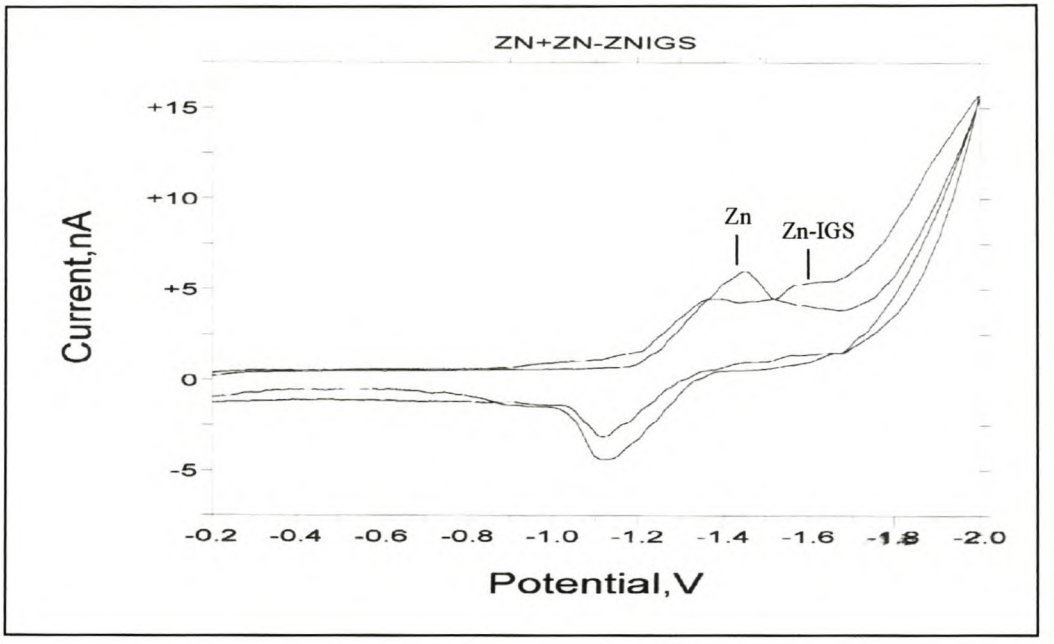


**Figure 21** Cyclic voltammogram of $Zn^{2+}$ and $Zn^{2+}$-IGS complex at pH of 10.3 and 9.6 respectively in 0.1 M ammonia buffer, T= 25°C, thin film mercury coated carbon electrode scan rate = 100 mV/s

Figure 21 represents the combined cyclic voltammogram of the zinc ions at Zn(Hg) and Zn-IGS metal ligand complex in the ratio of 1:1 ion solution observed at the potential of -1.45 and –1.57 V respectively. The complex peak was observed after the addition of aliquots of the appropriate ligand standard solution (0.01 M IGS) to the metal standard solution ($3.33 \times 10^{-4}$ M) in an electrochemical cell. The peak at -1.57 V corresponds to the reduction potential of the complex. After the complex formation, the peak height of

the zinc ion was observed to decrease, implying the involvement of some zinc ions in the complex formation with the ligand. Thereafter aliquots of 0.1 M HCl were added and the behaviour of the metal:ligand complexations was studied at different pHs. An analogous approach was used in the determination of the formation constants, as represented in section 3.4.1.5. Figure 22 represents a plot of ΔE vs pH for the Zn-IGS system.

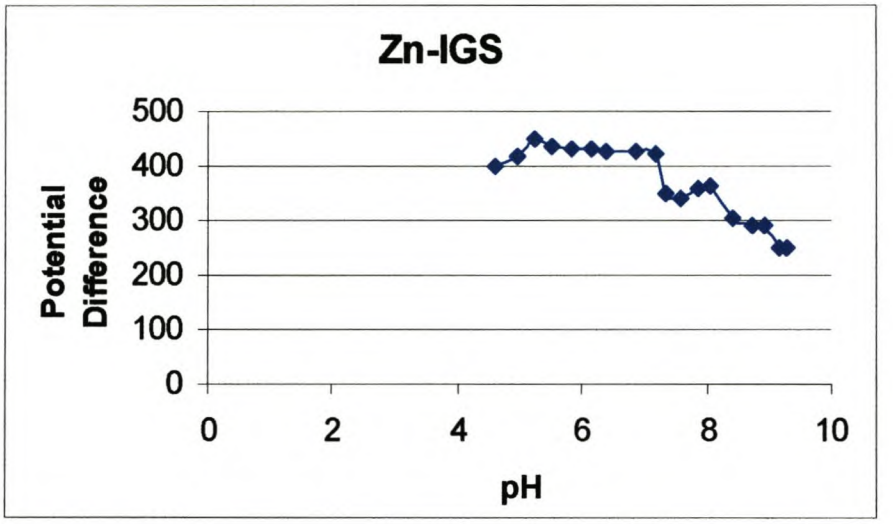


**Figure 22** Plot of ΔE vs. pH for determination stability constants, in pH 10.3 ammonia buffer (I=0.1 M, T = 25°C)

The major changes in the graph are at 5.23, 7.17, 7.58 and 8.05, which corresponds to the step-wise formation constants, $\log K_1$, $\log K_2$, $\log K_3$, and $\log K_4$ respectively. The over all formation constant, $\log K_f$, is the summation of the step-wise formation constants, which is equal to 28.03. This value is larger than the corresponding ZnIDG complex, showing that the trend predicted by Crouch et al [21], in their theoretical semi-empirical molecular orbital study of complex stabilities, holds.

### 3.4.3.1.1 Study of Cadmium(II) and its IGS complex

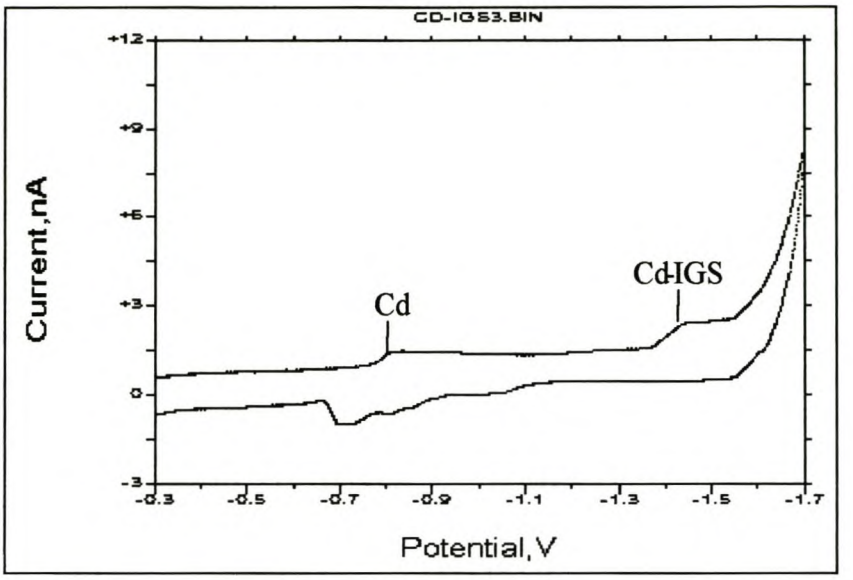


**Figure 23** Cyclic voltammogram of $Cd^{2+}$-IDG at pH 10.2 in 0.1 M ammonia buffer, T= 25°C,thin film mercury coated carbon electrode scan rate = 100 mV/s

The cyclic voltammogram for the $Cd/Cd^{2+}$ redox couple is given in figure 32, in the appendix. Figure 23, which was obtained after the addition of an appropriate amount of ligand solution, depicts the voltammogram for the $[Cd\text{-}IGS]^{2-}$ complex. During the cathodic sweep a peak was observed at a potential of -1.45 V, which corresponds to the reduction potential of the complex Cd-IGS. 0.1M HCl solution was used to study the step wise and simultaneous decomplexation and protonation process of the complex. A plot of the ΔE vs pH the different species obtained at different pH's in figure 24.

From this graph, it is observed that a change in the slope of the ΔE against pH curve

signifies a change in the major components of the different species of Cd with the complex. This value is larger than the value obtained for Cd-IDG complex.

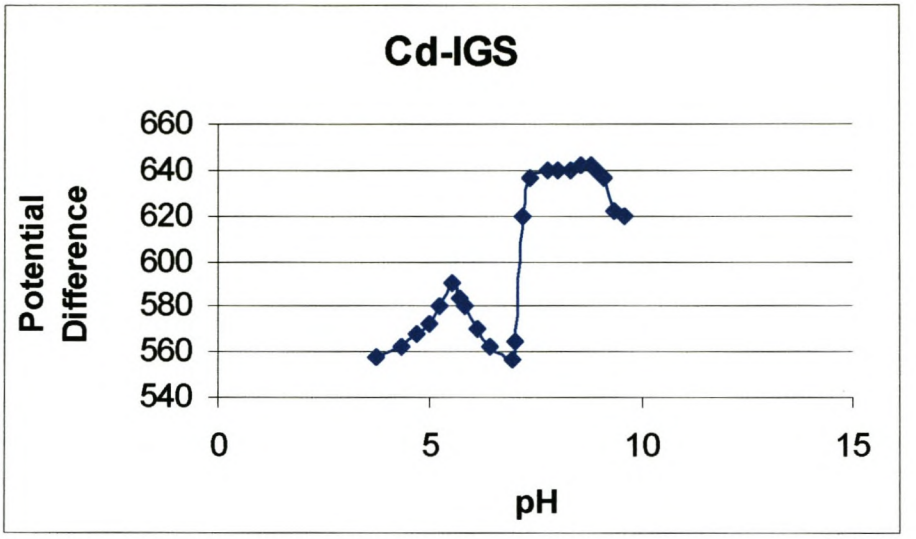


**Figure 24** Plot of ΔE vs. pH for determination of stability constants, in pH 10.3 ammonia buffer (I=0.1 M, T = 25°C)

These major changes were observed at, 5.5, 6.93, 7.4, and 8.58, which up on addition gives us the overall formation constant, $\log K_f = 28.41$, of the $[Cd\text{-}IGS]^{2-}$ complex.

#### 3.4.3.1.1 Study of Copper (II) and its IGS complex

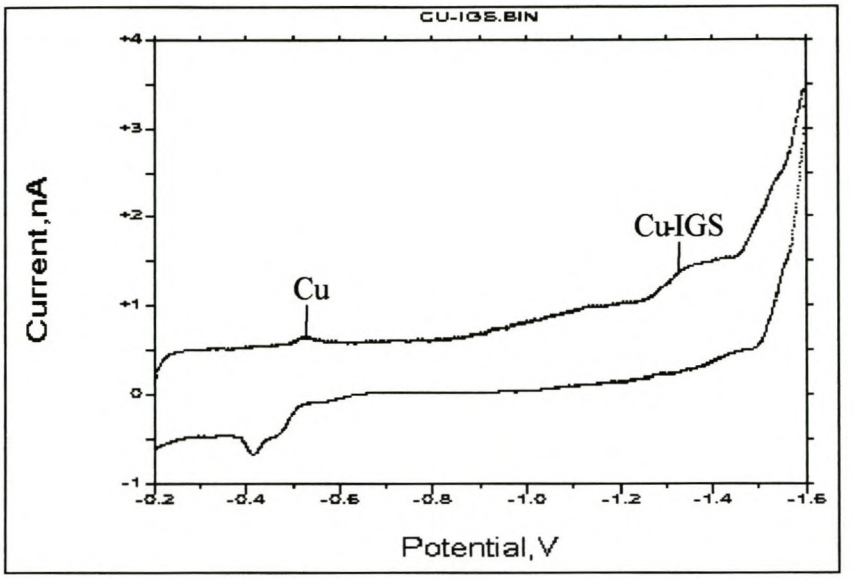


**Figure 25** Cyclic voltammogram of $Cu^{2+}$-IDG at pH 9.4 in 0.1 M ammonia buffer, T= 25°C,thin film mercury coated carbon electrode scan rate = 100 mV/s

A quasi-reversible cyclic voltammogram of $Cu/Cu^{2+}$ can be found in the appendix (Figure 33). Shown in Figure 25 is the voltammogram for the $[Cu\text{-}IGS]^{2-}$ complex. At a potential of –1.33 V the electrode becomes sufficiently strong enough to reduce the copper complex. At this potential the peak for the complex was observed and hence it is the reduction potential of the complex. Construction of a distribution curve yielded figure 26.

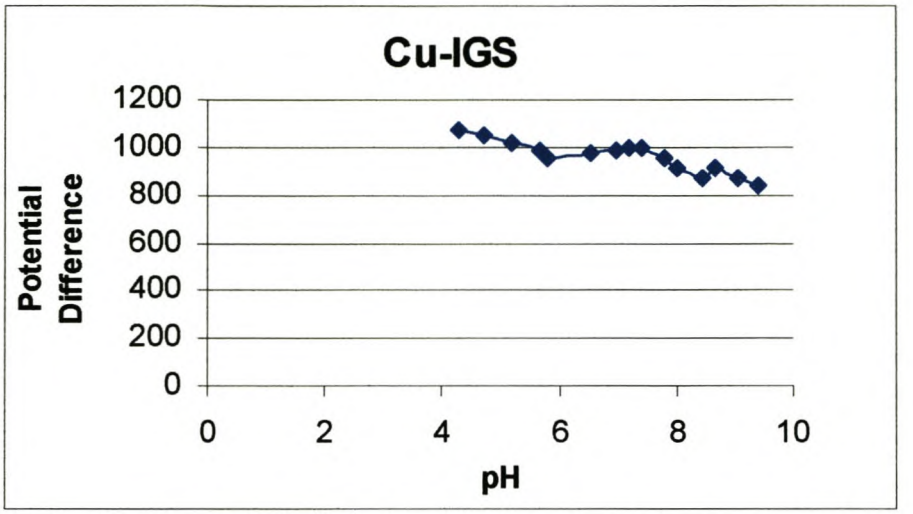


**Figure 26** Plot of ΔE vs. pH for Cu-IGS stability constants determination, in pH 10.3 ammonia buffer (I=0.1 M, T = 25°C)

From the graph four major changes in the gradient can be seen at 5.82, 7.41, 8.42 and 8.67, which depict the different species of the copper species at these pHs. This corresponds to the step-wise formation constants of the complex. The overall formation constant of the Cu-IGS complex is, $\log K_f = 5.82 + 7.41 + 8.42 + 8.62 = 30.32$.

| Metal Ion | Peak Potential (mV) | | |
|---|---|---|---|
| | Metal Ion | Metal Ligand* Complex | ΔE |
| **Copper (II)** | -508 | -1333.7 | 825.7 |
| **Cadmium** | -985 | -1446.6 | 461.6 |
| **Zinc (II)** | -1447 | -1569.3 | 122.3 |

* The ligand is IGS

**Table 6** Peak potentials for free metal ions and metal-IGS complexes

| Metal | Logarithm of the Stability Constants | | | | |
|---|---|---|---|---|---|
| | $logK_1$ | $LogK_2$ | $LogK_3$ | $LogK_4$ | $\Sigma logK_f$ |
| $Zn^{2+}$ | 5.23 | 7.17 | 7.58 | 8.05 | 28.03 |
| $Cd^{2+}$ | 5.5 | 6.93 | 7.4 | 8.58 | 28.41 |
| $Cu^{2+}$ | 5.82 | 7.41 | 8.42 | 8.64 | 30.32 |

**Table 7** The complex stability constants of $Zn^{2+}$, $Cd^{2+}$ and $Cu^{2+}$ with $H_4IGS$

| Ligands | Metals | | |
|---|---|---|---|
| | Zn $LogK_f$ | Cd $LogK_f$ | Cu $LogK_f$ |
| IDG | 20.10 | 21.70 | 23.21 |
| IGS | 28.03 | 28.41 | 30.32 |

**Table 8** Comparison of formation constants between IDG and IGS complexes with the selected metal ions.

As in the case of the IDG complexes, with the three selected metal ion, IGS gave the same trend in the order of the values of the formation constants. The relative stability of the 1:1 metal complexes were found to increase in the order of Zn-IGS < Cd-IGS < Cu-IGS, which is roughly in agreement with the Irving-Williams order of stability for complexation between transition metal ions and chelating agents. (Refer the Irving-Williams order on page 67 the footnote)

Comparison of formation constants between IDG and IGS complexes with the selected metal ions is given in table 8. When compared, the values of the stability (formation) constants of the two ligand complexes, the IGS ligand shows a greater affinity for the

selected metals. This is related to the size of the rings in the complexes formed between the ligands and the selected metal ions. In other words, the size of the chelate ring formed has a bearing upon the stability of the complex. The most common, and therefore the most stable, transition metal chelates are five-membered and six-membered rings (counting the metal atom). Five-membered rings frequently appear to be favoured when the atoms of the rings are linked by single bonds only. [21] IDG- iminodiglutaric acid, has got longer N-bonded alkanoate side chains ligators when compared to the IGS- iminoglutaricsuccinic acid- side chain ligators. IDG, when complexed with transition metal ions, four, six-membered rings are formed while a five-membered ring and three six-membered rings are formed in the case of IGS. The five-membered ring in IGS is expected to increase the stabilization of the complex formed when compared to the IDG complexes with similar metals in aqueous media. Theoretical indications of complex stabilities, according to Crouch et al. [20], in the case of the crystalline complexes, increase with an increase in the number of 6-membered rings formed upon complexation, i.e. complexation is favoured with an increase in the length of the side chain ligator. In aqueous media, i.e. in solutions, the stability trends increase as the side chain ligator decreases.

## 3.5 References


1. J.M. Bobbitt, P.J. Wills, *J. Org. Chem.*, 1980, **45**, 1978
2. T.K. Peter, R.H. Williams, *J. Chem. Edu.*, 1983, **60**, 702-706
3. V.M. Stackelberg, H.Z.V. Freyhold,. *Electrochem*, 1940, **46**, 120
4. J.Lingan, *J. chem. Rev.*, 1941, **29**, 1
5. D.D. Deford, D.N. Hume, *J. Am. Chem. Soc.* 1951, **73**, 5321
6. W.B. Schaap, D. L. McMasrers, *J. Am. Chem. Soc.*, 1961, **83**, 4699
7. J. M. Powers, J.T. Meyer, *J. Amer. Chem. Soc.*, 1980, **102**, 1289
8. H.M. Killa, *J. Chem. Soc.* Faraday Trans 1, 1985, **81**, 2659
9. S.Pons, M. Fleischmann, *Anal. Chem.* **59**, 1987, 1391-1399
10. D.A Skoog, D.M West, J.F. Holler, Fundamentals of Analytical Chemistry, 1992, Saunders Collage Publishing, New York.
11. N.V. Rees, J.A. Alden, R.A. W. Dryfe, B.A. Coles, R.G. Compton, *J. Phys. Chem.*, 1995, **99**, 14913-14818
12. T. Maloy, *J. Chem. Edu.*, 1983, **60**, 285-289
13. J. Wang, *Analytical Electrochemistry*, VCH Publisher Inc., New York, 1994.
14. A.J. Bard, L.R. Faulkner, *Electrochemical Methods; Fundamentals and Application*, John Wiley and Sons, New York, 1980
15. G.A. Mabbott, *J. Chem. Ed.*, 1983, **60**, 697-701

**16.** A.M. Crouch, L.E. Khotseng, M. Polhuis, D.R. Williams, *Analytical Chemical Acta,* 2001, **448**, 231-237

**17.** I. Cukrowsk, *Electroanalysis*, 1997, **9**, 167-1173

**18.** I. Cukrowsk, M. Adsetts, *J. Electroanal. Chem*., 1997, **429**, 129-137

**19.** R.W. Okey, S. Lin, P.K.A. Hong, *Emerging Technologies in Hazardous Waste Management* 7, Plenum Press, New York, 1997

**20.** A.M. Crouch, M. Polhuis, *Theochem*, 2000, **530**, 171-176

**21.** J. Kleinberg, W.J. Argersinger, E. Griswold, *Inorganic Chemistry*, D.C. Health and Company, Boston, 1960

# Chapter Four

## Concluding Remark

# 4 Concluding Remarks

The two new APCA ligands IDG and IGS were synthesised, in their tetrasodium salt form, in fairly good yields and good purity from relatively quite expensive starting materials, in three steps. The precursor, commercially unavailable, for both ligands, ethyl β-aminoglutarate, was also synthesized in three steps. The spectroscopic analysis and melting point measurement of the precursor was in good agreement with the literature values. The complete hydrolysis reaction, removal of the four ethyl groups, from iminodiglutarate and iminoglutaratesuccinate was performed successfully. The key to identifying an ethyl ester, the quartet around 4.0 ppm and the associated triplet at 1.2 ppm in the $^{1}$H-NMR spectra of the iminodiglutarate and iminoglutaratesuccinate were eliminated on hydrolysis. The peak of the solvent, methanol, used during the hydrolysis reaction of the ethyl esters, appeared as a singlet at δ 3.3 in both $^{1}$H-NMR spectra for both ligands. The solvent can simply be removed by carefully drying, the solid product, in vacuum.

An electrochemical study was conducted on the IDG and IGS complexes with selected transition metal ions ($Zn^{2+}$, $Cd^{2+}$ and $Cu^{2+}$) using cyclic voltammetry. The values of the formation constants of the complexes were found to be larger when compared to other widely used (e.g. EDTA and EDDS) APCA complexes. Hence it can be concluded that, IDG and IGS have better complexing ability (affinity) towards these metals.

Comparing the two ligands, IGS was found to have greater affinity towards the selected transition metal ions. This is due to the fact that stabilization of complexes, in aqueous media, increases with the decrease of the side chain ligators.

## Avenues for Further Works

Due to the time constraints, the following experiments were not conducted. In future the following experiments should be done:

- Biodegradability test on the ligands
- Elemental analysis of the ligands
- Crystalline Complex growth and crystallography (X-ray diffraction) study
- Determination of formation constants of metal ligand complexes using other methods (e.g. Potentiometric Method) to validate the CV results.
- Speciation study using capillary electrophoresis (CE).....

# 5 Appendix

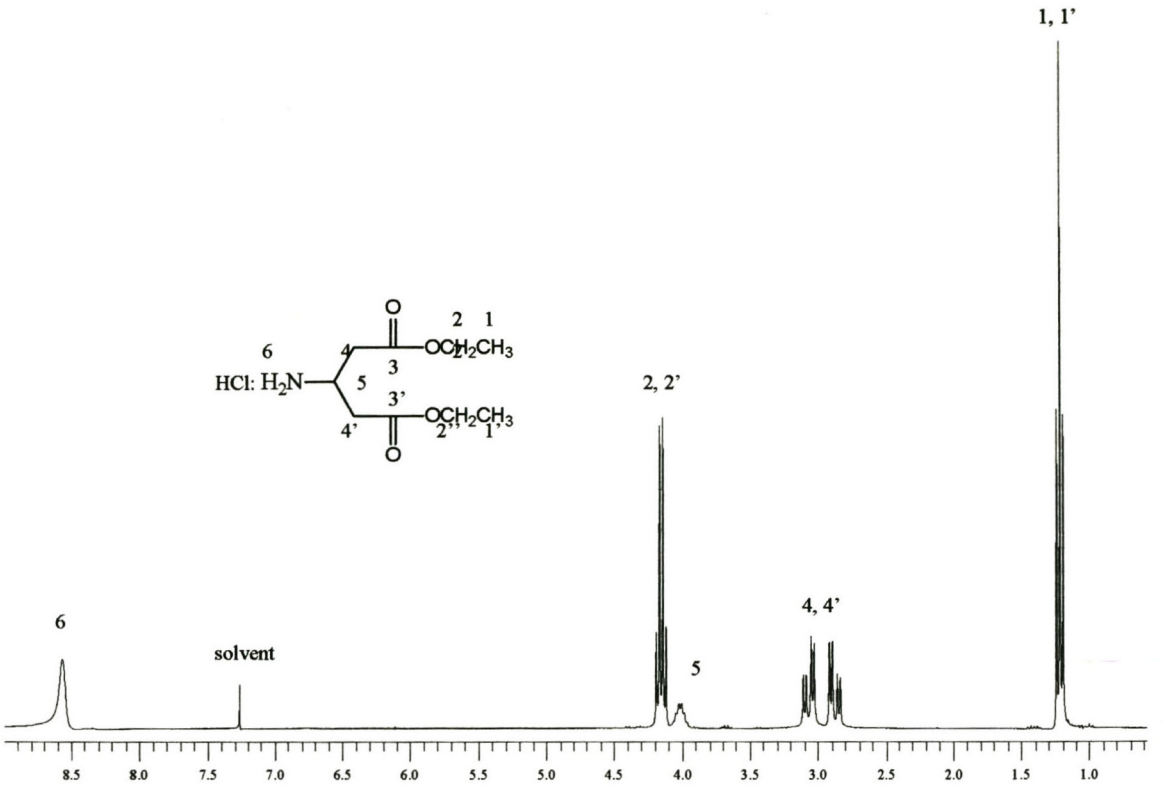


**Figure 27** $^{1}$H-NMR spectrum of ethyl β-aminoglutarate hydrochloride, obtained from the 300 MHz NMR-instrument, $CDCl_3$ as a solvent and TMS as internal reference

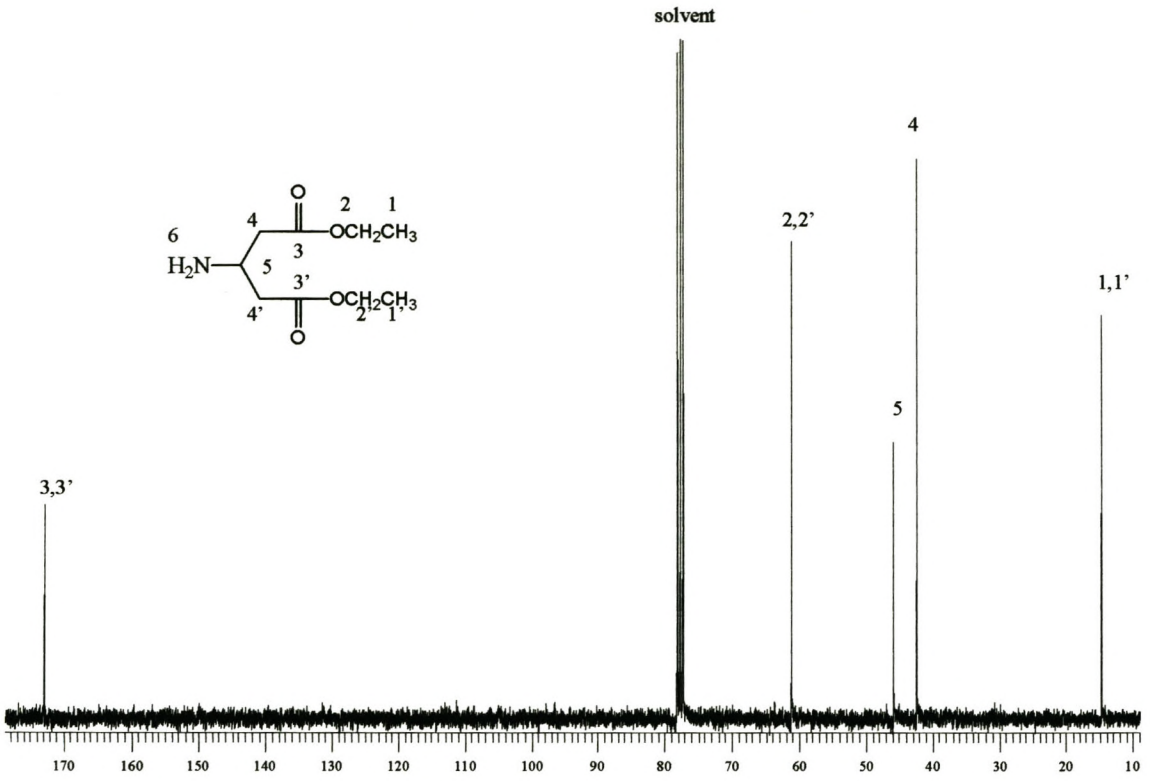


**Figure 28** $^1$H-NMR spectrum of ethyl β-aminoglutarate obtained from the 300 MHz NMR-instrument, $CDCl_3$ as a solvent and TMS as internal reference

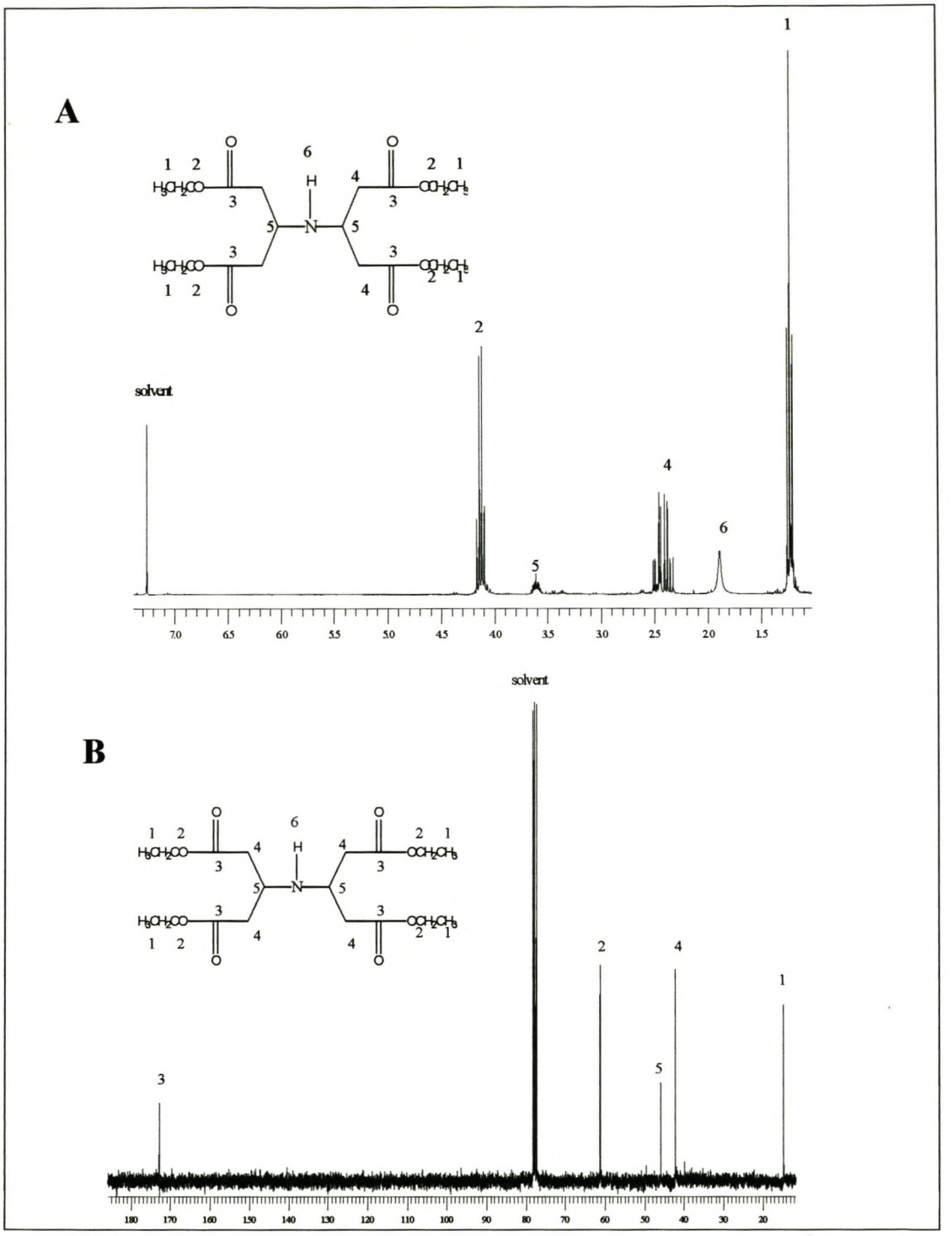


**Figure 29** **(A)** $^{1}$H-NMR spectrum of tetraethyl iminodiglutarate; (B) $^{13}$C-NMR spectrum of Iminodiglutarate both obtained from the 300 MHz NMR-instrument, $D_2O$ as a solvent.

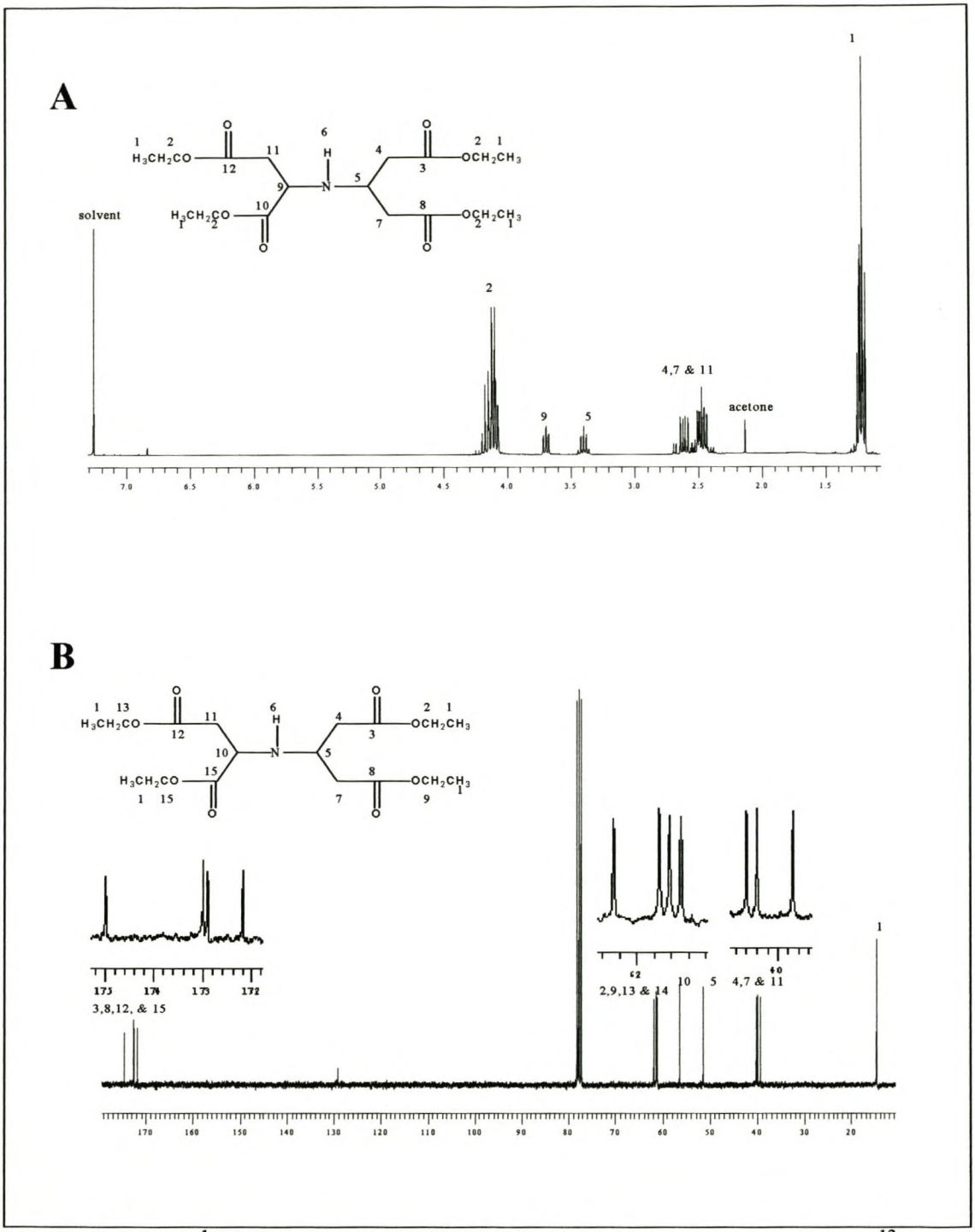


**Figure 30** **(A)** $^{1}$H-NMR spectrum of tetraethyl iminoglutaratesuccinate **(B)** $^{13}$C-NMR spectrum of Iminoglutaratesuccinate. Both obtained from the 300 MHz NMR-instrument, $CDCl_3$ as a solvent.

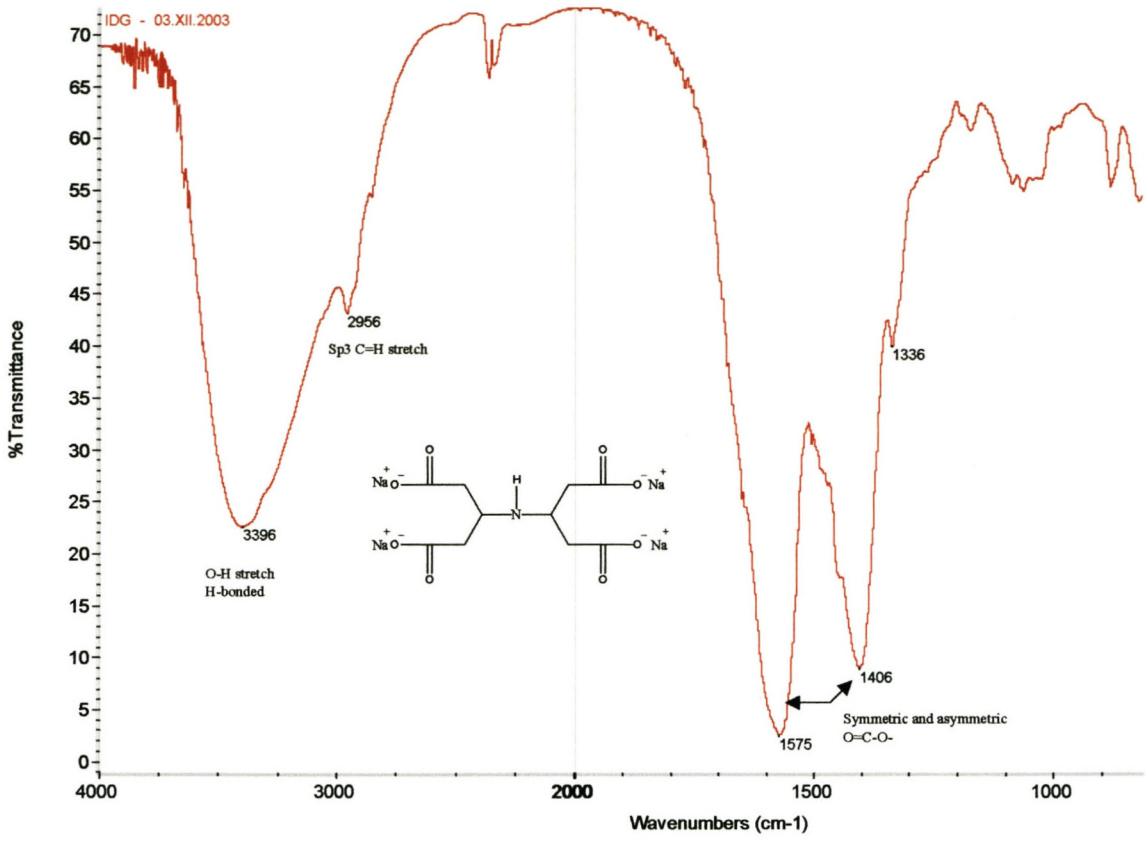


**Figure 31** IR spectrum (KBr plate) for the IDG-4Na

Cyclic voltammograms obtained for the metal ions during the metal:IGS complexation study are presented below.

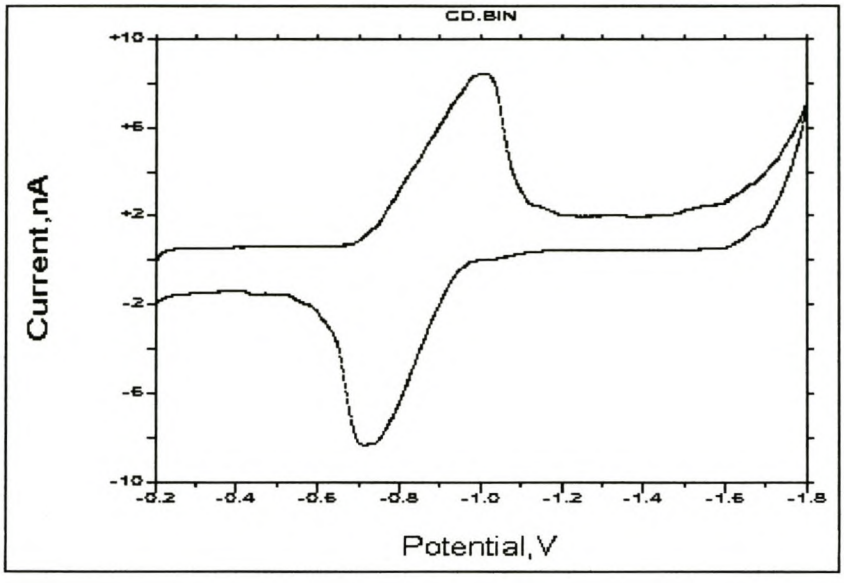


**Figure 32** Cyclic voltammogram of Cd at pH 10.3, in 0.1 M ammonia buffer, T = 25°C, thin film mercury coated carbon microelectrode; scan rate = 100 mV/s

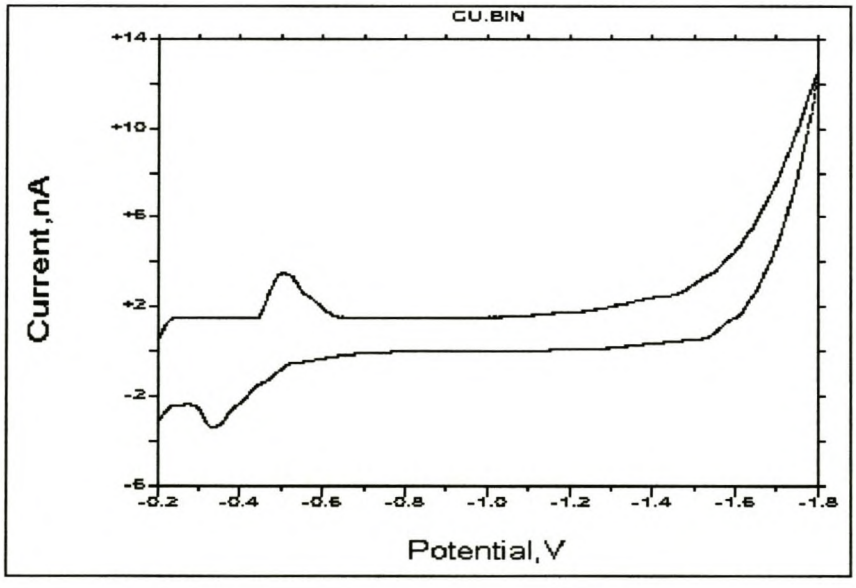


**Figure 33** Cyclic voltammogram of Cu at pH 9.8, in 0.1 M ammonia buffer, T = 25°C, thin film mercury coated carbon microelectrode; scan rate = 100 mV/s